Environmental Science and Pollution Research
https://doi.org/10.1007/s11356-018-1679-x

RESEARCH ARTICLE

Long-term trends in Swiss rivers sampled continuously over 39 years reflect changes in geochemical processes and pollution

Juerg Zobrist[1,2] · Ursula Schoenenberger[1] · Simon Figura[1,3] · Stephan J. Hug[1]

Received: 7 April 2017 / Accepted: 4 March 2018

Abstract

Long-term changes of 14 water constituents measured in continuously and water discharge proportionally collected samples of four Swiss rivers over a period of 39 years are analyzed using several statistical techniques. Possible drivers and causes for the identified trends and shifts are explained by consideration of catchment characteristics and anthropogenic activities. Water temperatures increased by 0.8–1.3 °C, whereas water discharges remained largely unchanged. Concentrations of alkalinity, total hardness, Ca, and Mg regulated by dominant carbonate lithologies in catchments increased by up to 10%. We attribute this change to an increase in the partial pressure of CO_2 in the subsurface, provoked by increasing temperatures. Re-oligotrophication processes in lakes also influence the behavior of alkalinity and silicic acid. In contrast to concentrations, most loads did not change significantly, due to their large variances. Therefore, no changes in overall weathering rates of carbonate rocks can be detected. The outgassing of CO_2 in rivers from the place of carbonate dissolution to measurement stations amounts up to 6% (mean) of CO_2 sequestered (mean 1.1 mol m^{-2} a^{-1}) by the weathering of rock minerals. Changes in alkalinity/Ca/Mg ratios indicate an increase in calcite precipitation over time. Total nitrogen concentrations and loads peaked at the end of the 1980s and then decreased up to 50%, while NO_3 concentrations showed almost no changes. This dynamic matches the changes in the agricultural N balance. Concentrations and loads of Na and Cl increased up to 60% due to an increase in the various uses of rock salt.

Keywords River · Long-term trends · Geochemical processes · Nitrogen pollution · Switzerland

Introduction

Evolution of river monitoring and water quality assessment

River monitoring in industrialized countries in the sense of regular surveillance of water constituents was initially implemented whenever river water use was impaired by pollution. A few citations may illustrate the history of such monitoring. The 140-year nitrate record of the River Thames represents one of the earliest and longest studies (Howden et al. 2010; Worrall et al. 2015). In Germany, the history of water surveillance of the Elbe and Rhine rivers started in the early nineteenth century (Schwandt et al. 2010). After World War II, riparian countries of the Rhine started a common river monitoring program (the International Commission for the Protection of the Rhine (Mostert 2009) and the International Working Group of Public Water Supply Companies using Rhine Water (IAWR; http://www.iawr.org). The concept of the US National Water Quality Assessment (NAWQA) Program refers to 100 years of water quality data collection by the US Geological Survey (Hirsch et al. 1988). Monitoring data relating to chemical and biological conditions in the highly impacted and small Glatt River documents the evolution of pollution and of protection measures taken in Switzerland starting in 1933 (Zobrist et al. 2011). All these cited river surveillance programs, as well as numerous national programs, started in the 1970s, collect grab samples in more or less regular time intervals, mostly monthly. This sampling

Responsible editor: Philippe Garrigues

Electronic supplementary material The online version of this article (https://doi.org/10.1007/s11356-018-1679-x) contains supplementary material, which is available to authorized users.

✉ Stephan J. Hug
stephan.hug@eawag.ch

Juerg Zobrist
juerg.zobrist@emeriti.eawag.ch

[1] Eawag, Swiss Federal Institute of Aquatic Science and Technology (Eawag), 8600 Dübendorf, Switzerland

[2] Present address: Uster, Switzerland

[3] Present address: Zürich, Switzerland

Published online: 03 April 2018

procedure introduces a notable uncertainty in the calculation of fluxes (loads) due to diurnal, weekly, and seasonal fluctuations in flow and particularly during flood events. Numerous methods with extended discussions have been published to determine the "best and realistic" flux in rivers from concentrations in grab samples and more frequently measured water discharge, for example (Hirsch 2014; Worrall et al. 2013, and references therein).

In the last 20 years, river monitoring has been expanded to integrated water quality management especially by including ecological assessments, as in the European Water Framework Directive (WFD) OJL 327 (22 December 2000, pp. 1–73; http://ec.europa.eu/environment/water/water-framework/index_en.html or in the revised Swiss law on Water Protection of 1991 https://www.admin.ch/opc/en/classified-compilation/19910022/index.html.

The realization of integrated water quality management relies on a profound knowledge of drivers governing water quality and on data characterizing the catchments and their water regimes in detail (Hirsch et al. 2006; Bundi et al. 2000b).

Analyzing the time series of geochemical water constituents obtained from long-term river monitoring programs has attracted recent interest and has revealed changes in local and global cycles of geogenic elements. For example, changes in dissolved inorganic carbon fluxes to the oceans may affect the global biogenic carbon cycle and the sequestration and release of CO_2 by rivers and lakes (Raymond and Cole 2003; Perrin et al. 2008; Raymond et al. 2008; Worrall et al. 2012; Stets et al. 2014; Lauerwald et al. 2015 and others).

Aim of this study

In the present work, we systematically analyze a 39-year dataset of the National Long-term Surveillance of Swiss Rivers (NADUF) program consisting of physical indicators, of the most important geochemical water constituents and of the main nitrogen species. We apply several statistical methods to visualize and quantify long-term changes in concentrations and loads (fluxes). No best-fit method for determining loads is needed, since the sampling technique produces continuous water discharge-weighted samples. Time series are tested for monotonic trends, abrupt changes, and similarities. These statistical results combined with a detailed knowledge of the Swiss environmental system provided the basis for the identification of drivers and causes of detected changes. Possible drivers, such as anthropogenic inputs and global warming, might affect geochemical processes, such as weathering rates, CO_2 sequestration, CO_2 evasion, and mineral equilibria. Our data evaluation centers on four large Swiss catchments of the rivers Rhine, Rhône Aar, and Thur. The present work includes the most recent datasets of the monitoring program and analyzes the long-term data series in a more comprehensive manner than earlier evaluations cited below.

Methodology and methods

The National Long-Term Surveillance of Swiss Rivers monitoring program

In Switzerland, the renewed water protection law established in 1971 mandated an improved river-monitoring program for chemical constituents. At the beginning of 1974, a novel sampling system was implemented that allowed the collection of integrated, water discharge-weighted samples over periods of 1 or 2 weeks. With this type of continuous and water-discharge proportional sampling, proper mass flows (loads, fluxes) can be determined.

The NADUF program https://www.bafu.admin.ch/bafu/en/home/topics/water/state/water–monitoring-networks/national-surface-water-quality-monitoring-programme–nawa-/national-river-monitoring-and-survey-programme–naduf-.html was launched to evaluate the effectiveness of water protection measures at the federal level and to survey changes in the water composition of representative Swiss rivers. In addition, the data obtained in the NADUF program substantially increased the scientific value of the hydrological information base of the country.

Sampling stations are located along the main rivers of the country that represent the headwaters of important Central European rivers, particularly the Rhine and the Rhône. Stations are also situated along tributaries of large lakes bordering the Alps, at the Swiss border, and along selected smaller rivers. Since the beginning of the program, several data evaluations have been performed in various contexts and have been published as listed on the NADUF homepage. Using NADUF data, it was possible to quantify the effects of protective and curative measures, such as the marked decrease in phosphorus loads in Swiss rivers and lakes after the ban of phosphates in laundry detergents in 1986 (Siegrist and Boller 1999; Jakob et al. 2002; Zobrist and Reichert 2006). The alpine rivers are less affected by anthropogenic inputs but exhibit unique characteristics, such as low nutrient exports and higher physical than chemical weathering rates. These results add valuable information about processes in less populated areas (Zobrist 2010). Extended discussions of the temporal trends of dissolved and total organic carbon in the main rivers have revealed the complexity involved in interpreting small changes (Rodriguez-Murillo et al. 2015).

The NADUF sampling system also simultaneously provides samples for specific studies with different targets, such as the monitoring of heavy metals (Zobrist et al. 2004), micropollutants (Stoll and Giger 1998; Ahel et al. 2000; Giger et al. 2006), isotopes (Schuerch et al. 2003), or herbicides (Moser et al. 2017).

The NADUF program is integrated in the national surveillance of surface water quality https://www.bafu.admin.ch/nawa which includes the cantonal surveillance programs and which is based on a modular concept (Bundi et al. 2000a). Data obtained

from the permanent and temporary NADUF stations can be retrieved from http://www.eawag.ch/en/department/wut/main-focus/chemistry-of-water-resources/naduf/.

Stations

This study analyzes data from seven NADUF stations situated on the rivers Rhine, Rhône, Aar, and Thur (Fig. 1). The chosen stations have been in operation continuously for 30 to 39 years, resulting in time series of about 780 to 1000 biweekly data points per station. The main characteristics of the catchments and the time periods under examination up to 2013 are shown in Table 1. The two border stations, Village-Neuf/Weil (VW) on the Rhine and Chancy (CH) on the Rhône, represent the main water outflow of Switzerland. In each of these two catchments, approximately 76% of the out-flowing water has its source in the country. Together, they represent 85% of the total Swiss water export. Regarding area, approximately three quarters of each catchment area are located in Switzerland. Together, these parts of catchments make up 86% of the Swiss territory (41,285 km^2). In terms of inhabitants, in each catchment approximately 78% of the population lives in Switzerland, making up 95% of the total Swiss population (8.1 million, 2012). The partition features and the geomorphology shown in Fig. 1 indicate that the Swiss contribution determines the character of the two rivers at the two border stations.

Catchment characteristics (attributes)

Climate

The catchments are situated in a temperate-humid climatic zone with higher precipitation rates in summer than in winter. Estimated precipitation rates in the catchments studied varied from 1.2 to 1.4 $m^3\ m^{-2}\ a^{-1}$ ($m\ a^{-1}$). Measured water discharge of the rivers averages between 0.9 and 1.2 $m\ a^{-1}$. These discharges are larger than those in the US Appalachian rivers https://pubs.usgs.gov/of/1987/ofr87-242, e.g., Mohawk River 0.57 $m\ a^{-1}$ (Godwin et al. 2003), or those in lowland European rivers, e.g., Rhine River mouth 0.36 $m\ a^{-1}$, River Elbe 0.15 $m\ a^{-1}$. https://www.iksr.org/wasserrahmenrichtlinie/bewirtschaftungsplan-2015.

The important water sources of the rivers are situated in the alpine and peri-alpine regions, which exhibit low evapotranspiration rates. These regions are covered by snow in the winter; as a result, water discharge peaks early in summer. The water discharge of rivers situated downstream of the lakes, the Rhône at Chancy (CH), the Rhine at Rekingen (RE), the Aar

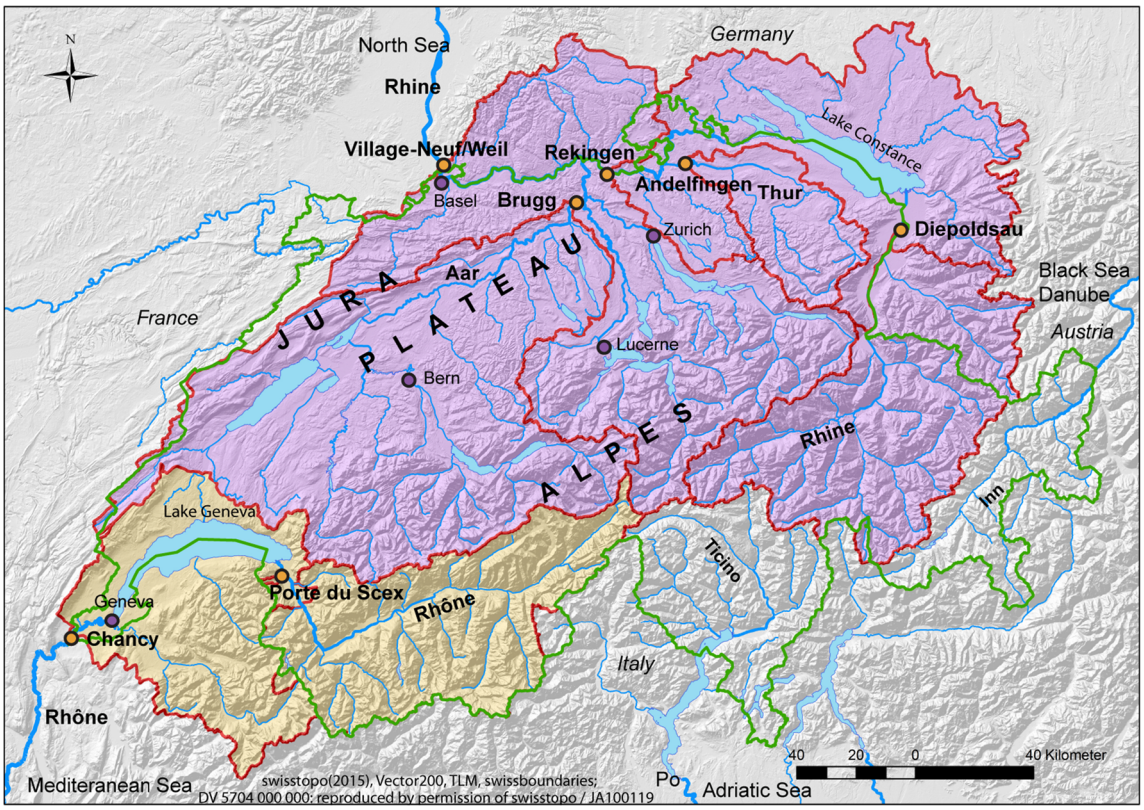

Fig. 1 Geomorphologic map of Switzerland and the location (orange filled circles) of the seven stations of the NADUF program selected for the present study. The red lines delimit river catchments. The Swiss border is shown in green. The purple background marks the Rhine catchment and the yellow background the Rhône catchment

Table 1 Sampling stations, catchment area, land uses, water discharge, average altitude, inhabitants in the catchment area, and start of sampling

River	Station[a] and abbreviation	Catchment area (km^2)	Land use in % (2012)[b]				Water Discharge sample period ($m^3 s^{-1}$)	Average altitude of catchment (m.a.s.l.)[d]	Inhabitants estimated 2012 in 1000	Sampled since
			Agricultural intensively used land	Extensively used vegetation covered	Dense forest	Barren land				
Rhine	Village-Neuf/Weil[c] VW	36,472	32	21	29	11	1084	1100	7600	1977
	Rekingen RE	14,718	30	25	27	11	450	1260	2800	1976
	Diepoldsau DI	6119	8	47	25	17	232	1800	340	1984
Rhône	Chancy CH	10,294	14	24	25	30	353	1580	1700	1978
	Porte-du-Scex PO	5220	6	32	19	40	188	2130	310	1975
Aar	Brugg BR	11,750	36	18	28	11	323	1010	2200	1975
Thur	Andelfingen AN	1696	52	11	26	2	48	770	380	1982

[a] Information about station coordinates (http://www.hydrodaten.admin.ch/en/)

[b] The sum of different land uses does not make up 100% because the contribution of settlements and traffic areas has not been listed

[c] 1995, Rhine station Village-Neuf was transferred 2.7 km upstream to Weil

[d] Stations altitudes vary between 244 and 410 m.a.s.l.

at Brugg (BR), and the Rhine at Village-Neuf (VW) responds only slowly to heavy rainfalls. In contrast, the alpine rivers Rhône at Porte-du-Scex (PO) and Rhine at Diepoldsau (DI) and the pre-alpine river Thur at Andelfingen (AN) show clear peak flows. Presently, rivers in their lowland area are almost entirely channelized and often hold hydropower stations. Nevertheless, the rivers exhibit a clear water flow velocity and turbulence that result in nearly 100% mean oxygen saturation; see the NADUF webpage.

Lithology

The underlying bedrock and the unconsolidated zones of the catchments studied consist mainly of Mesozoic limestone (calcite and dolomite, with Triassic intrusions of anhydrite/gypsum). Zones with crystalline rocks and schist (slate) formation, so-called "Bündner Schiefer," predominate in some alpine headwater areas, particularly in the Rhône catchment (Gnägi and Labhart 2017). Due to historic glaciations, most soils around the Alps are relatively young (< 12,000 years B.P.). The most developed soils are Cambisols and Luvisols covering the drained and rather stable areas.

Land use

Land uses in the different catchments vary considerably (Table 1). Areas with intensive agriculture (meaning heavily fertilized land) consist of about two thirds of grasslands utilized for dairy and animal farming, and one third of arable land, producing various crops. These types of areas make up little of the alpine catchments, but occupy nearly half of the Thur catchment and contribute significantly to diffuse inputs of N and P into rivers (Zobrist and Reichert 2006). The unfertilized areas, which are covered by vegetation and are extensively used, e.g., as alpine grasslands, bush land, and parks, are more common in the alpine regions. The percentage of barren land (no vegetation and surface waters) varies considerably. The fraction of areas with dense forests of a mix of deciduous and coniferous trees, depending on altitude and forest management, varies moderately. The inputs from the last three types of land use represent approximately the natural input of nutrients and geochemical constituents. Over the past 30 years, the changes in land uses were limited. Urban land, which occupies only a minor fraction of the country, has increased distinctly at the cost of agricultural land. However, these changes, as well as shifts in the partition of uses and of crops planted, are modest. The catchments of the stations situated at the Swiss border include some areas of neighboring countries; see Fig. 1. These areas exhibit comparable geomorphologic and structural properties as Switzerland. Therefore, the land use characteristics extrapolated from the Swiss part of the catchment result in a reasonable characterization of the whole catchment.

Pollution

The potential pollution impact by the population can be expressed as a percentage of wastewater produced in relation to the mean water discharge. It varies from 0.6% in the alpine Rhône to 2.8% in the Thur, assuming 300 L of wastewater per capita per day. The estimation of the total N load of the wastewater input to surface waters suggests that this load has not changed substantially since 1980; results of evaluated loads are listed in Suppl. Table 5. The higher overall pollution load caused by the population growth from 6.2 to 8.1 million in Switzerland and the increased connection of sewers to treatment (70% in 1975 to nearly 100% in 2013) was compensated approximately by the more efficient N elimination in treatment plants. Unfortunately, there exists hardly any data that clearly indicates a decrease in the overall discharge of N with wastewater into rivers, which was achieved successively by the introduction of denitrification processes in treatment plants in the past 10 years.

Fertilizer containing reduced N species (N_{red}), especially manures, may produce strong acid in soils, thus dissolving the carbonate minerals and producing alkalinity. Overall in Switzerland, the use of manures and mineral N fertilizers has decreased by 17 kt N (11%) and by 25 kt N (33%) (Spiess 2011) since 1990, resulting in a decrease of approximately 1.60 and 2.35 g N m^{-2} to intensively used agricultural land. This reduction in fertilizer use is the result of a politically induced obligation imposed to farmers. According to this obligation, farmers should limit the use of fertilizers according to the requirement for a fair crop yield in relation to the quantity and timing of fertilizer applications in regard to the available stock of N in the soil.

Liming of agricultural land, i.e., application of calcareous material, is rarely implemented, since most soils are located over unconsolidated calcareous rocks or moraines. https://www.bfs.admin.ch/bfs/de/home/statistiken/raum-umwelt/ressourcen/umweltindikatorensystem/emissionen-und-abfaelle/stickstoffbilanz.assetdetail.324482.html.

Over the last 30 years, the average atmospheric deposition of sulfur over Switzerland decreased significantly from approximately 46 to 6 mmol m^{-2}. This distinct reduction is due to the decline of sulfur dioxide emissions in middle-European and especially in Eastern-European countries (Berge et al., 1999). The deposition of oxidized N diminished from 50 to 35 mmol m^{-2}, and that of N_{red} decreased only slightly from 85 to 72 mmol m^{-2} http://www.emep.int/mscw/mscw_data.html. The decrease in the N_{red} load and the increase of the pH in the wet deposition (Federal Office for the Environment 2015) have reduced the total acidifying atmospheric inputs by 60 mmol H^+ m^{-2} over the last 30 years. https://www.bafu.admin.ch/bafu/de/home/themen/luft/publikationen-studien/publikationen/nabel-luftqualitaet-2016.html.

In contrast to many industrialized countries, Switzerland has only a few large industrial plants with large emissions of pollutants.

The neighboring countries have undertaken similar efforts to reduce pollution as those made by Switzerland; therefore, the changes in the Swiss areal pollution loads are representative for the entire catchments at the border stations.

Sampling and analytical methods

Sampling

For the data presented in this study, continuous, biweekly samples were collected. Each sample consists of thousands of subsamples, which are taken proportionally to the water discharge of the river. The unique sampling apparatus is described in detail in the Suppl. Material. It provides a water discharge-weighted concentration in each sample analyzed.

The examined concentration distributions in the cross sections of the rivers are almost uniform in respect to the location of the intake. Therefore, the samples taken are representative for the river at the station, except for small deviations at the stations Village-Neuf and Weil. The relocation of station Village-Neuf 2.7 km upriver to the international Rhine surveillance station at Weil (Ruff et al. 2013) may have provoked small shifts of geochemical parameters. However, these minimal changes do not influence the results of our evaluation.

Water discharge, water temperature, and pH are measured continuously on-site at the sampling station.

Measurements, analytical methods, and data processing

Immediately after arrival at Eawag, a portion of each sample is filtered (using a washed 0.45-μm cellulose-nitrate filter). The filtered and unfiltered portions are stored at 4 °C until analysis. The water constituents measured in the 2-week-integrated samples examined in this study are alkalinity (Alk), total hardness (TH), Ca^{2+}, Mg^{2+}, Na^+, K^+, SO_4^{2-}, Cl^-, silicic acid (H_4SiO_4), NO_3^-, and total nitrogen (TN). The methods used conform to the ISO/EN methods for water analysis and are summarized in http://www.eawag.ch/en/department/wut/main-focus/chemistry-of-water-resources/naduf/.

All measured data in the monitoring program are subject to extensive quality control procedures before transfer into the data bank. Considering the effect of the concentration smoothing in continuously collected samples, strongly deviating and non-plausible values were deleted. The influence of modifications in analytical methods has been re-examined carefully in the context of this work, as described in the assessment report of analytical modification in the Suppl. Material. The continuously and online measured parameters water discharge, water temperature, and pH were averaged over the exact time period of each water sampling. Overall, the long-term

NADUF dataset can be considered reliable and consistent in terms of sampling, analytics, and data treatment.

Time series analysis

The Seasonal Mann–Kendall test (results not shown) and an earlier data evaluation using a combined sinusoidal and linear regression revealed significant seasonal fluctuations and trends (Zobrist et al. 2004). Based on studies of the detection and the estimation of changes in water quality by Esterby (1996) and Hirsch et al. (1991), we have chosen a method that separates seasonality and smoothes long-term changes as best suited for our study. To comprehensively assess the long-term changes in the time series, we applied additional statistical methods designed to detect significant monotonic trends and abrupt changes (shifts), as explained below. Where possible, the calculations were implemented with the corresponding programs of the statistical open source software R (R Development Core Team 2011), available from http://stat.ethz.ch/CRAN. The methods used are as follows.

The seasonal trend decomposition procedure based on local regression

STL is an iterative non-parametric procedure developed by Cleveland et al. (1990) that considers every value, measured in a time series with a constant time interval of observation, as a sum of three interpretable components: (1) the seasonal component (high-frequency part), (2) the trend component, that is, the long-term change (low-frequency part), and (3) the remainder component (random variation = residual). The STL method estimates the smoothed long-term fluctuation and the seasonality by local regression (LOESS), which can be visualized graphically. The best-suited smoothing parameters (window widths) for the simulation were 1 year for the seasonality and 5 years for the long-term fluctuation, corresponding to 27 and 130 data points. A distinct longer smoothing period, such as 10 years, would mask meaningful information. In our work, we denote the values estimated for the low-frequency component (long-term change) as the 5-year STL trend component.

The STL procedure cannot be applied if data points are missing. For most of the chemical parameters studied, missing data amounted to only 0.5 to 2% for the four stations DI, PO, RE, and VW, with hardly any sampling interruption. However, 5 to 11% of the biweekly observation data were missing at the three stations BR, AN, and CH, due to interruptions caused by reconstruction work. Total nitrogen often exhibits a higher quota of non-available data than the other parameters. In order to process these datasets, missing chemical data was interpolated using the non-parametric projection pursuit regression procedure.

Projection pursuit regression

In principle, this method is based on a linear combination of a non-linear transformation of explanatory variables (Friedman and Stuetzle 1981). In our case, water discharge, water temperature (both also measured during times of missing data), date, month, and differences in the water discharge from previous dates were used as predictors for missing data. Values modeled with PPR fit visually very reasonably into the gaps of time series; see the example in Suppl. Fig. 1. Therefore, PPR is a well-founded interpolation technique for producing continuous and complete time series for analysis by STL. Additionally, PPR can be used as an additional quality control method to assess odd values.

Estimation of the linear long-term changes and trends

The slopes of the linear trend in the time series were estimated using the parametric linear regression of the STL 5-year trend components, as visualized in Figs. 3 and 7. The small skewness in the distribution of the STL trend components, as displayed in Suppl. Fig. 2, does not affect the results of the linear regression calculation (Suppl. Tables 1a and b). The statistical significance of coefficients was assessed according to the counts of years instead of the counts of data points, in order to account for the autocorrelation in the time series of the STL 5-year trend component. Slopes were estimated for the period from 1983 to 2013, consisting of about 900 data points. This period represents the longest common interval for all seven stations, thus enabling a proper comparison of the time series analyzed.

STARS test for abrupt shifts

To identify abrupt changes (regime shifts) in time series, the sequential t test analysis between means of data segments (STARS test) (Rodionov 2004) was applied to annual means and biweekly data. The chosen segment length was 10, with a significance level of $p = 0.01$. The STARS tests were also used to detect artificial synchronous shifts in concentration time series provoked by a modification in analytical methods, as presented in the Suppl. Material "Report analytical methods."

Confidence intervals of the STL trend component

The confidence intervals (Conf I) of the 5-year STL trend component of time series were estimated as the propagated error sum of the 95% confidence interval for the analytical error and for the standard deviation (stdev) of the STL remainder (Eq. 1). Both confidence intervals were calculated for the count of observations in 5 years. This mode of calculation underrates the total confidence interval in the first and last 2-

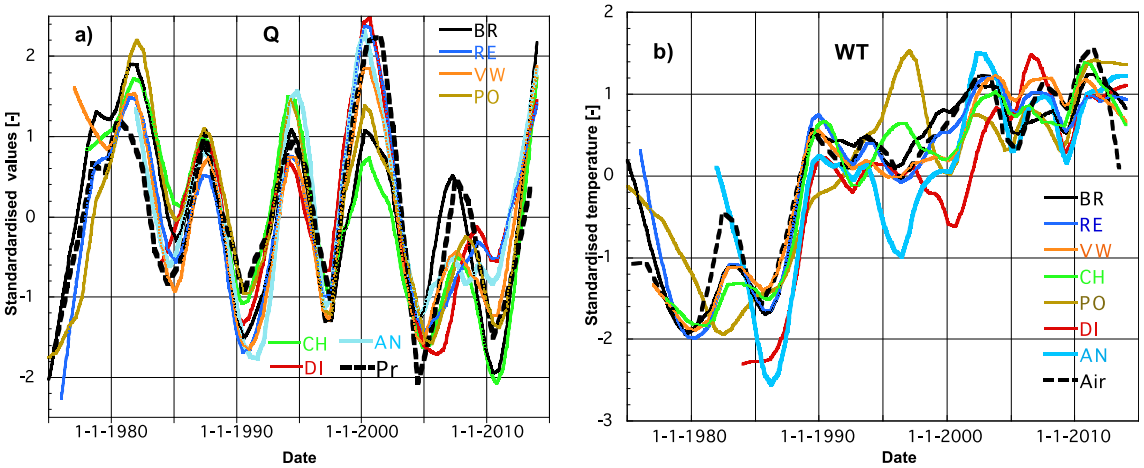

Fig. 2 Time series of standardized 5-year STL trend components **a** for water discharge (Q) and annual precipitation rate (Pr) and **b** for water temperature (WT) and annual air temperature (Air). For station abbreviations and mean water discharges, see Table 1. Mean water temperatures 1983–2013 in degree Celsius: Rhine stations, VW 12.5, RE 11.7, DI 8.0; Rhône stations, CH 11.6, PO 7.2; Aar station BR 11.9, Thur station AN 10.7. Mean air temperature of the 12 Swiss climatologic basis stations, 7.3 °C in the period 1983 to 2013

year period of the time series. However, it does not impact information contained in the graphs.

$$\text{Conf } I_{\text{total}} = \left((\text{Conf } I_{\text{anal error}})^2 + (\text{Conf } I_{\text{stdev rem}})^2 \right)^{1/2} \quad (1)$$

Standardization

To analyze the similarities of time series between rivers, standardized (normalized) values, z_i, for each 5-year STL trend component value, x_i, were calculated. They are obtained in relation to the arithmetic mean x_{av} of the whole STL trend time series and the standard deviation s_d (Eq. 2). The resulting values of z_i are displayed graphically as time series.

$$z_i = (x_i - x_{av})/s_d \quad (2)$$

Mineral equilibrium

The calculations of the mineral saturation states and of the calcite–carbon dioxide equilibrium were performed using the free equilibrium speciation model Visual MINTEQ, available at https://vminteq.lwr.kth.se/

Results and discussion

Water discharge and water temperature

Time series of the standardized 5-year STL trend components for water discharge depict a very similar fluctuation pattern at all stations (Fig. 2a). Linear regression indicates a significant yearly decrease for the Rhône at CH of 1.9 $m^3\ s^{-1}\ a^{-1}$ and for the Rhône at PO of 0.4 $m^3\ s^{-1}\ a^{-1}$ from 1983 to 2013 (Table 2). Decreases at the other stations are too small to be statistically significant. It is interesting to note that the two Rhône catchments exhibit a distinctly larger area of glaciation (8% at CH, 14% at PO) than the other catchments (0 to 2%). A detailed hydrological study would be needed to reveal unequivocal differences between catchments and to determine the causes. The synchronous pattern of fluctuations between water discharge and precipitation rate in Fig. 2a reflects the basic hydrological relationship between discharge and precipitation.

The curve characteristics of the STL 5-year trend components for water temperature (Fig. 2b) are less uniform than those of the water discharge among the rivers studied. Importantly, the water temperatures increased over time, with a distinct upward shift for all stations in the period from 1987 to 1989 (Fig. 2b). Long-term changes in the irregularly fluctuating curves depicted in Fig. 2b could be assessed by two statistical methods:

1. Applying linear regression over the whole period from 1983 to 2013: The increase of water temperature amounted to 0.027 ± 0.003 °C a^{-1} (i.e., 0.8 ± 0.1 °C in 30 years) in the alpine and peri-alpine rivers (Table 2), with no lakes in the catchment (stations DI, PO, and AN). For the other stations, which are situated downstream of large lakes, the slopes were between 0.035 and 0.044 °C a^{-1} (i.e., 1.0 to 1.3 °C in 30 years). Similar long-term linear rates of temperature increases were found in rivers situated in other regions of the world with comparable climate conditions, such as in England and Wales (Orr et al. 2015), in East coast rivers in USA (Kaushal et al. 2010), in Germany (Arona et al. 2016), and in Austria (Webb and Nobilis 2007). In the period from

Table 2 Statistically significant slopes estimated by the linear regression of 5-year STL trend components from 1983 and 2013

River	Station	Q ($m^3\ s^{-1}\ a^{-1}$)	WT ($K\ a^{-1}$)	TH ($\mu eq\ L^{-1}\ a^{-1}$)	Alk ($\mu eq\ L^{-1}\ a^{-1}$)	Ca ($\mu eq\ L^{-1}\ a^{-1}$)	SO_4 ($\mu eq\ L^{-1}\ a^{-1}$)	H_4SiO_4 ($\mu mol\ L^{-1}\ a^{-1}$)
Period		1983–2013						
Rhine	VW	–	+ 0.044***	− 2.8***	+ 3.1***	− 4.9***	− 3.3***	+ 0.28***
	RE	–	+ 0.038***	+ 6.6***	+ 7.4***	+ 3.4***	–	+ 0.36***
	DI	–	+ 0.026***	+ 3.5***	+ 5.4***	+ 2.5***	–	− 0.042**
Rhône	CH	− 1.9***	+ 0.038***	+ 1.8**	+ 2.7***	–	+ 1.4***	− 0.19***
	PO	− 0.43**	+ 0.024***	+ 6.1***	+ 4.0***	+ 4.1***	+ 4.0***	− 0.073*
Aar	BR	–	+ 0.035***	− 2.7*	+ 2.3**	− 4.5***	− 1.5***	+ 0.17***
Thur	AN	–	+ 0.030***	− 7.6***	− 3.7***	− 7.2***	− 3.9***	− 0.12*

River	Na ($\mu mol\ L^{-1}\ a^{-1}$)	Cl ($\mu mol\ L^{-1}\ a^{-1}$)	NO_3 ($\mu g\ N\ L^{-1}\ a^{-1}$)	TN ($\mu g\ N\ L^{-1}\ a^{-1}$	pH $10^{-3}\ a^{-1}$	Mg ($\mu eq\ L^{-1}\ a^{-1}$)	K ($\mu mol\ L^{-1}\ a^{-1}$)
Period	1983–2013				1995–2013	1983–1987 and 2010–2013	
Rhine	− 1.3*	− 1.7*	− 10***	− 34 ***	–	+ 1.3*	–
	+ 2.1***	+ 2.1***	–	− 19***	+ 4.6*	+ 1.6**	+ 0.13***
	+ 2.1***	+ 2.5***	–	− 13***	–	–	+ 0.11***
Rhône	+ 4.3***	+ 4.9***	+ 8.0***	− 9.0***	–	+ 1.2***	+ 0.28***
	+ 4.4***	+ 5.1***	–	− 15***	+ 6.0*	+ 0.87**	+ 0.58***
Aar	+ 3.4***	+ 1.3***	− 9.9***	− 32***	+ 4.6*	+ 0.85**	+ 0.12**
Thur	+ 3.2***	+ 4.8***	− 17***	− 52***	–	–	–

For parameters exhibiting a shift due to modifications in analytical methods, only those slopes of linear regression of 5-year STL trend components are shown, which were obtained in the period of trustable pH measurements or in the periods not measured with inductive couple plasma spectrometry (ICP). See the SI report. For station abbreviations, see Table 1

Statistical significance levels: *$p < 0.05$; **$p < 0.01$; ***$p < 0.001$

1990 to 2013, the increases were smaller; they varied between 0.017 and 0.035 °C a^{-1}, except at station PO where it was insignificant.

2. Quantifying changes as shifts, the STARS test indicated a significant upwards shift during the period from 1987 to 1989 of 0.41–0.54 °C in the alpine Rhine, in the Rhône, and in the subalpine river Thur, with no lakes in the catchment. At the station downstream of the lakes situated on the Swiss Plateau, the upwards shifts amount to 1.0–1.3 °C (Suppl. Table 2). These differences in shifts, as well as in linear increases per year, between river stations situated upstream and downstream of lakes (Fig. 1) point to the role of lakes (stagnant waters) in the warming-up surface waters. For example, in Lake Geneva, situated between stations PO and CH, the water temperature at a depth of five meters increased at a rate of 0.06 °C a^{-1} in the period from 1983 to 2013 (Barbier et al. 2017). Also a shift of about 0.7 °C from 1987 to 1989 can be observed visually. Abrupt water temperature increases in the late 1980s coincided with those found in other rivers, as well as in lakes across Switzerland (North et al. 2013) and in groundwater (Figura et al. 2011). In both types of water, the changes in water temperature occurred at the same time and the shifts ranged from 0.4 to 1.3 °C. An equivalent observation was made in soils at 10 meteorological stations; the local temperatures at a depth of 25 cm experienced an average upward shift of 0.7 K in 1988 (R.E. Hari, personal communication, November 2014). It is now established that the observed abrupt shifts in water and air temperature and in various parameters of other earth systems reflect a climatic regime shift over large areas occurring in the northern hemisphere in the late 1980s (Reid et al. 2015). In the context of these cited observations, it is interesting to note that the upward shifts in the alkalinity, NO_3, and total nitrogen concentrations coincided approximately with that of the water temperature.

The results obtained by the two statistical approaches indicate reasonably well that each method only treats one facet of the temperature evolution displayed in Fig. 2b.

In Fig. 2b, the evolution of the annual mean air temperature estimated for Switzerland, smoothed over 5 year by the LOESS procedure, was similar to those for water temperature, indicating that the rising water temperature is associated with the increase of the air temperature (Webb and Nobilis 2007; Reid et al. 2015) (http://www.meteoswiss.admin.ch/home/climate/swiss-climate-in-detail/Swiss-temperature-mean/Data-on-the-Swiss-temperature-mean.html).

At each station, the slopes of the monthly water temperature increases were significant from April to June and were higher than in the other months of the year (Suppl. Fig. 3). This finding goes along with the observation that evolution of plant growth or start of blossom has shifted into an earlier time of the year (http://www.meteoschweiz.admin.ch/home/klima/klimawandel-schweiz/vegetationsentwicklung/lange-phaenologische-beobachtungsreihen.html).

Geochemical water constituents

Weathering of the rock-forming minerals calcite, dolomite, anhydrite/gypsum, silicates, halite, and sylvine governs concentrations and loads of the main geochemical species alkalinity, Ca, Mg, SO_4, and H_4SiO_4, and to a lesser extent of K, Na, and Cl (Stumm and Morgan 1996; Drever 1997; Zobrist 2010; Szramek et al. 2011; Lauerwald et al. 2013 and others). These natural processes may be affected by diverse anthropogenic activities (Stets et al. 2014), such as the eutrophication processes in lakes (Mueller et al. 2015; Bürgi 2015), the use of fertilizer in agriculture (Perrin et al. 2008), the application of de-icing salt (Godwin et al. 2003; Raymond et al. 2008), the input of wastewater containing ammonia, atmospheric deposition (Kaushal et al. 2013), climate change (Lauerwald et al. 2013), and urbanization (Kaushal et al. 2013). Based on these factors of influence (drivers), which are rather well known in the river system studied (described in the "Catchment characteristics" section), we will comprehensively discuss the identified changes in concentrations and loads, particularly in regard to geochemical processes.

Trends in concentrations and loads

Figure 3 shows the time series of the 5-year STL trend components of concentrations for total hardness, alkalinity, Ca, Mg, SO_4, and H_4SiO_4. They represent the datasets in a summarized form, indicating concentration ranges and ratios (values are reported in Suppl. Table 4). Notable are the high concentrations of SO_4 in the Rhône at stations PO and CH and in the alpine Rhine station Di. They are due to dissolution of gypsum/anhydrite deposits in the Bündner schist formations of the catchments. The sum of Ca, Mg, alkalinity, and SO_4 concentrations accounts for approximately 90% of the ionic content. At the measured pH conditions (Table 4) observed, alkalinity embodies almost completely the hydrogen–carbonate concentration HCO_3^- (Stumm and Morgan 1996). The smoothed time series of concentrations in Fig. 3 depict irregular fluctuations and changes over the measuring period, which are clearly larger than the 95% confidence intervals. Overall, nearly all concentrations of these geochemical species exhibited a small but statistically significant and mostly positive linear increase (trend) in the range of a few microequivalent per liter per area from 1983 to 2013 (Table 2). These trends correspond to a change of 0.6 to 3‰ per year for total hardness, alkalinity, and Ca, respectively, and up to 8‰ per year for SO_4, H_4SiO_4, and Mg. For comparison, many rivers in the Eastern US and in the Mississippi catchments also exhibit an increase in alkalinity,

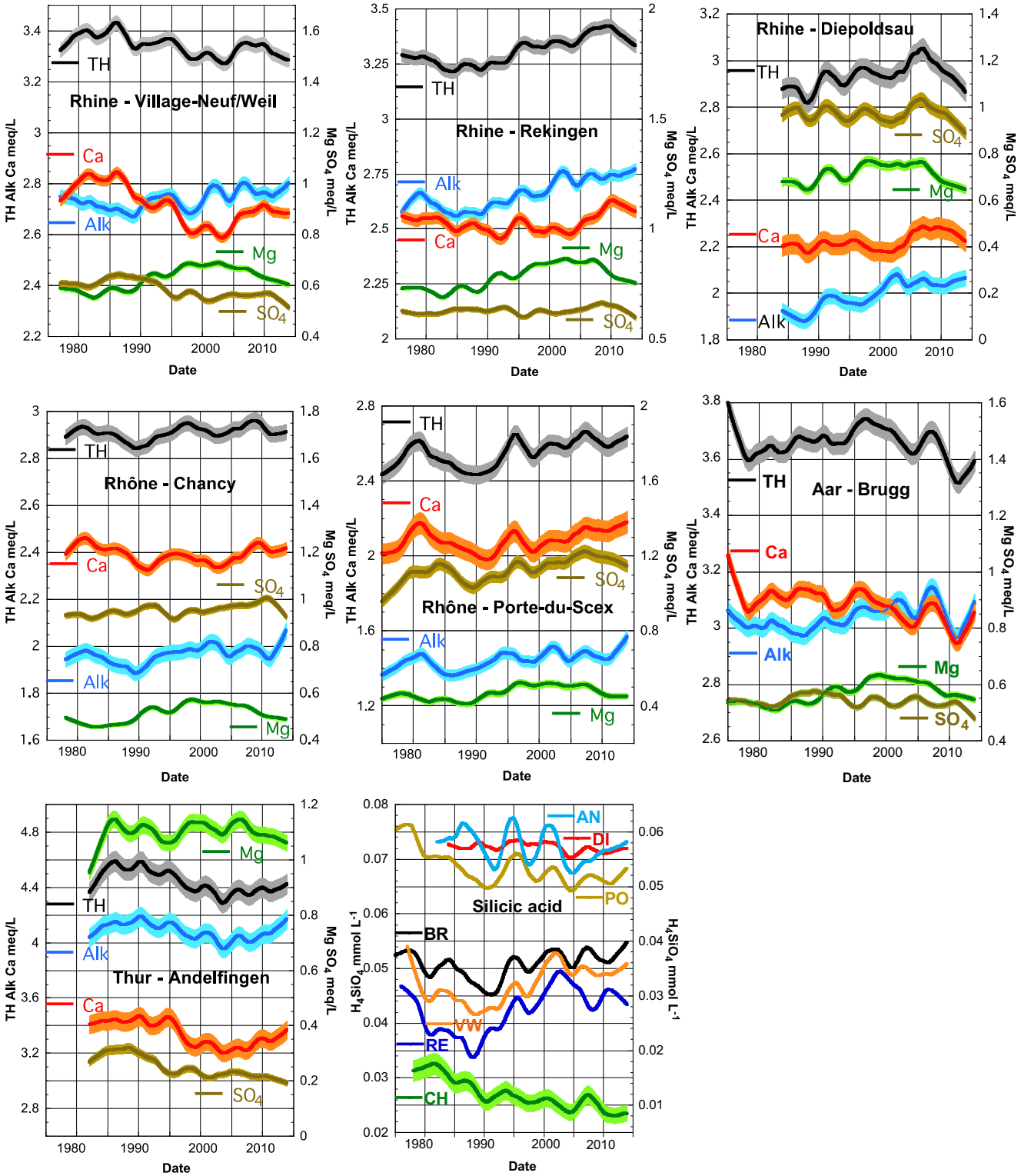

Fig. 3 Time series of 5-year STL trend components for the concentration of geochemical parameters: total hardness (TH), alkalinity (Alk), calcium (Ca), magnesium (Mg), sulfate (SO_4), and silicic acid (H_4SiO_4), visualizing the long-term changes and fluctuations. Shaded areas represent 95% confidence interval. Note: H_4SiO_4: for stations An, PO, and PO (station upstream lakes) scale on the right. Confidence intervals not shown are in the same range as indicated for station Chancy. The x-axis labels refer to the first day of the year (as in Fig. 2)

often at a higher linear rate than that stated in Table 2 (Kaushal et al. 2013; Stets et al. 2014; Raymond et al. 2008, and others). In the Thames River, the reconstructed increase in Ca concentrations is in the range of those reported in Table 2 (Worrall

Table 3 Statistically significant changes in annual loads estimated by the linear regression of 5-year STL trend components taken in relation to the arithmetic means

River	Station	TH (‰ a^{-1})	Alk (‰ a^{-1})	Ca (‰ a^{-1})	SO_4 (‰ a^{-1})	H_4SiO_4 (‰ a^{-1})	Na (‰ a^{-1})	Cl (‰ a^{-1})	NO_3 (‰ a^{-1})	TN (‰ a^{-1})	Mg (‰ a^{-1})	K (‰ a^{-1})
Period		1983–2013									1983–1987 and 2011–2013	
Rhine	VW	–	–	–	− 5.3***	+ 6.7*	− 2.5**	− 5.0*	–	− 18***	+ 0.14**	–
	RE	–	–	–	–	+ 9.8**	+ 8.3***	+ 9.8***	–	− 10***	+ 0.73**	+ 5.3***
	DI	–	–	–	–	–	+ 15***	+ 26***	–	− 17***	–	+ 5.5**
Rhône	CH	− 4.9*	− 4.3*	− 5.3***	− 4.0***	− 12**	+ 12***	+ 15***	6.6**	− 15***	–	–
	PO	–	–	–	–	− 3.8***	+ 11***	+ 17***	–	− 20***	–	+ 13***
Aar	BR	–	–	–	− 4.3**	–	+ 9.9***	–	− 7.0**	− 16***	–	–
Thur	AN	–	–	–	− 15***	–	+ 10***	+ 13***	− 6.0*	− 16***	–	+ 3.6**

For parameters exhibiting a shift due to modification in analytical methods, significant slopes in the "non ICP period" are taken; see report in Suppl. Material. For abbreviations of stations, see Table 1. Slopes, relative to the average load, are stated in order to compare rivers having different water discharges

*$p < 0.05$; **$p < 0.01$; ***$p < 0.001$

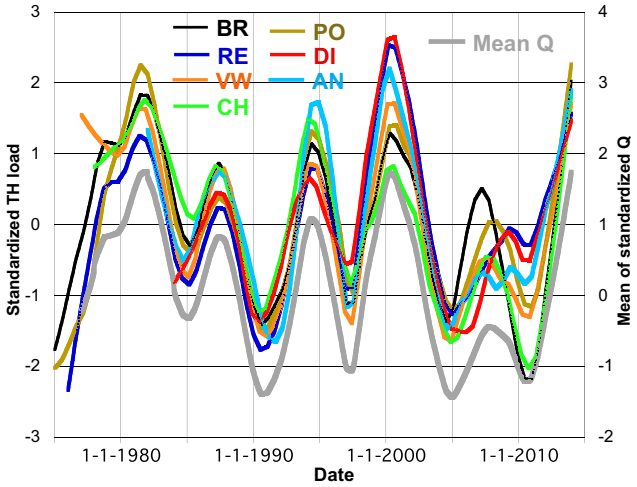

Fig. 4 Time series of standardized 5-year STL trend components of load for total hardness (TH) and the mean of standardized 5-year STL trend components of water discharge (Q) for all seven stations. For station abbreviations, see Table 1. Note: the right-side *y*-axis is shifted to depict the congeneric behavior of water discharge and load of total hardness

et al. 2012). These authors state that various anthropogenic drivers, such as agricultural practice, recovery of acidification, and changes in catchment attributes such as land use and cultivation or urbanization, are responsible for the observed changes in alkalinity and Ca.

Concerning abrupt shifts, only alkalinity indicated a small upward shift in the range of 1% in the years between 1989 and 1991 (Suppl. Table 2), which does not substantially affect the numerical values of the slopes cited above. Also noteworthy is that the shifts in alkalinity continued for 1 to 2 years after the increase of the water temperature.

The changes of loads, expressed as slopes of linear regression (Table 3), were less often statistically significant than those of concentrations. The combined effect of the variances in concentration and especially in water discharge (see Figs. 2a and 4) distinctly increases the statistical requirement for a significant slope in the regression calculation. However, if changes were significant, they can be substantial, for example, the changes at station CH and the changes in Na, Cl, and total nitrogen at most stations, as discussed in more detail below.

At all stations, the standardized time series of 5-year STL trend components of loads for geochemical species displayed an oscillation similar to that of water discharge, as shown exemplarily for total hardness in Fig. 4. It indicates the determining factor of the water discharge in the long-term changes of loads for geochemical species. The transport limitation for alkalinity has been shown and discussed for the Mississippi river by Raymond et al. (2008).

The time series with yearly means of loads of geochemical species do not exhibit abrupt shifts. The STARS test does not indicate a significant shift due to the strong variation in loads displayed in Fig. 4.

Table 4 Mineral equilibria of calcite, dolomite, and quartz: (a) changes of mean concentrations observed from the period 1995–1999 to the period 2009–2013, estimated H_2CO_3 concentrations in river waters, and saturation indices (SI); (b) changes of means observed from the period 1980–1984 to the period 2009–2013 (DI 1978–1988, AN 1982–1986) and changes of "native H_2CO_3" estimated for SI, calcite = 0. (Ca-SO4) represents the part of Ca dissolved by calcite and dolomite

(a)

		pH	H_2CO_3	H_4SiO_4	Calcite	Dolomite	Quartz
River	Station		µmol L^{-1}	µmol L^{-1}	SI	SI	SI
Rhine	VW	8.08 » 8.09	56 » 56	47 » 49	+ 0.41 » + 0.43	+ 0.15 » + 0.17	− 0.16 » − 0.15
	RE	8.14 » 8.20	49 » 44	44 » 46	+ 0.43 » + 0.51	+ 0.24 » + 0.41	− 0.18 » − 0.17
	DI	8.14 » 8.15	39 » 40	58 » 56	+ 0.18 » + 0.22	− 0.27 » − 0.22	0.00 » − 0.02
Rhône	CH	8.09 » 8.06	42 » 45	25 » 23	+ 0.24 » + 0.20	− 0.30 » − 0.34	− 0.41 » − 0.46
	PO	8.10 » 8.17	32 » 28	53 » 51	− 0.02 » + 0.06	− 0.83 » − 0.70	− 0.03 » − 0.05
Aar	BR	8.02 » 8.08	73 » 62	51 » 52	+ 0.46 » + 0.49	+ 0.09 » + 0.15	− 0.11 » − 0.11
Thur	AN	8.19 » 8.24	67 » 60	57 » 57	+ 0.73 » + 0.78	+ 0.88 » + 0.99	− 0.05 » − 0.05

(b)

		WT	Alk	Ca-SO_4	Mg	H_2CO_3 "native"
River	Station	°K	meq L^{-1}	meq L^{-1}	meq L^{-1}	µmol L^{-1}
Rhine	VW	11.44 » 12.88	2.71 » 2.77	2.22 » 2.14	0.57 » 0.62	127 » 131
	RE	10.75 » 12.01	2.59 » 2.75	1.91 » 1.97	0.71 » 0.78	100 » 118
	DI	7.43 » 8.20	1.89 » 2.05	1.22 » 1.32	0.67 » 0.67	34 » 44
Rhône	CH	10.62 » 12.04	1.97 » 1.98	1.51 » 1.44	0.46 » 0.50	50 » 48
	PO	6.70 » 7.54	1.46 » 1.48	1.00 » 0.97	0.43 » 0.46	16 » 17
Aar	BR	11.04 » 12.24	3.01 » 3.00	2.58 » 2.47	0.52 » 0.56	178 » 173
Thur	AN	10.20 » 10.89	4.12 » 4.10	3.12 » 3.10	1.08 » 1.08	370 » 367

(c)

		CO_2 outgassed mmol per m^2 catchment area per year		CO_2 outgassed mol per m^2 river area per year
		Δ Flux model	Diffusion model	Diffusion model
		"native place" to river station	River station to atmosphere	River station to atmosphere
River	Station			
Rhine	VW	68	192	85
	RE	70	159	55
	DI	5	97	40
Rhône	CH	3	164	55
	PO	− 13	34	12
Aar	BR	89	259	96
Thur	AN	268	306	90

Description of Δconcentration model and diffusion model; see "CO_2 outgassing from rivers" section. All calculations were performed using Visual MINTEQ

Mineral equilibria of alkalinity, Ca, Mg, and H_2CO_3 in water

The chemical equilibrium calculations using Visual MINTEQ for the weathering reactions (Suppl. Table 3) indicated a 1.5- to 6-fold (except at PO) supersaturation for calcite in river waters (Table 4 (a)). This represents a well-known phenomenon in waters originating from carbonate lithologies (Drever 1997; Szramek and Walter 2004 and others). A supersaturation factor of less than 1 log unit can usually persist in river waters and does not provoke fast calcite precipitation (Szramek and Walter 2004). In winter, supersaturations were slightly higher and in summer slightly lower than the means in Table 4 (not shown). The saturation index for the mineral "dolomite ordered" indicated a small supersaturation or undersaturation depending on the river. The saturation index for "dolomite disordered" always remained in a high state of undersaturation (not shown). As pH and water temperature were increasing, the supersaturation of calcite and dolomite also increased, except at station CH. At all stations, the equilibrium concentration of CO_2 in river water (H_2CO_3) was 1.5- to 3.6-fold oversaturated with respect to the equilibrium of atmospheric CO_2 with water (Table 4 (a)). These CO_2 concentrations ranged between 17 and 20 μmol L^{-1} (corresponding to pCO_2 of −3.452 atm, Mount Loa, Hawaii) depending on the mean water temperature of the river.

The next point of discussion refers to chemically reactive CO_2 in the subsurface. Equilibrium calculations by Visual MINTEQ allow estimating the H_2CO_3 concentration in the subsurface where the initial dissolution of minerals occurs, denoted here as "native H_2CO_3." This concentration can be regarded as the minimum average concentration of H_2CO_3 (equivalent to the partial pressure of CO_2, pCO_2) needed to achieve measured concentrations of alkalinity, Ca, and Mg by the dissolution of calcite and dolomite. It presents a proxy for the average H_2CO_3 in the subsurface (soil, aquifer) for which hardly any data exists. The "native H_2CO_3" concentration, that is, pCO_2, is calculated at the equilibrium condition where the saturation index of calcite equals zero. For this evaluation, corrected concentrations of Ca minus SO_4, Ca_{corr}, have to be used. Ca_{corr} represents the part of Ca that results from the dissolution of calcite and dolomite. The part of Ca due to the gypsum/anhydrite dissolution does not count in this approach. The contribution of silicate weathering to the Mg and Ca concentrations is small and can be ignored, because of the dominant carbonate lithology; see also "Chemical weathering rates" section. At the chemical condition of "native H_2CO_3," the measured Mg concentrations indicated a distinct undersaturation with respect to dolomite. The measured increases in water temperature, alkalinity, Mg (Table 2), and Ca_{corr} (Suppl. Table 4) resulted in a slight increase in "native H_2CO_3" at some stations (Table 4 (b)). This increase reflects the effects of intensified microbial degradation activities and accelerated plant growth, due to the temperature increase in soil and groundwater, as has been documented by Macpherson et al. (2008). These authors have reported a 20% increase in the modeled partial pressure of CO_2 in an undisturbed karst aquifer in the period from 1991 to 2005. They did not provide a clear forcing mechanism, but they have suggested a strong influence of enhanced soil respiration. Time series showing increasing concentrations of alkalinity and total hardness in unconfined aquifers not recharged by rivers in the Canton of Zürich in Switzerland corroborate the hypothesis of increasing subsurface "native H_2CO_3" concentrations (www.awel.zh.ch/internet/baudirektion/awel/de/wasser/messdaten/gw_qualitaet.html#s-dosten).

Drivers responsible for changes in alkalinity and Ca concentrations

Taking the rivers studied into consideration, we suggest that two drivers may have promoted the increase of the long-term concentrations of alkalinity and Ca and one driver has promoted their decreases as documented below.

1. The increased microbial activities in the subsurface, caused by increased temperature, has led to slightly increasing "native H_2CO_3" concentrations, which give rise to higher concentrations of alkalinity, Ca, and Mg in the equilibrium with calcite and dolomite.
2. At stations downstream of lakes, the re-oligotrophication process in lakes also contributed to the alkalinity and Ca increases. The well-established decrease in phosphate concentrations in Swiss lakes has lowered the production of phytoplankton, which reduces the calcite precipitation induced in the lake. As a consequence, epilimnetic concentrations of alkalinity and of Ca are increasing (Mueller et al. 2015). In the Lower Lake Constance (western arm of the lake), the alkalinity and total hardness have risen significantly in the top layer 0 to 5 m by 3.8 resp. 3.5 μeq L^{-1} a^{-1} from 1996 to 2014 (H. Ehmann, Water Protection Office, State Thurgau, personal communication, December 2015). These changes were in the same range as those in the downstream Rhine station RE (Table 2). At station RE, about 80% of the water originates from the upstream Lake Constance (surface area 571 km^2, water volume 51 km^3, water residence time 4.3 a). In Lake Geneva (surface area 580 km^2, water volume 89 km^3, water residence time 11.3 a), located in a geographically similar situation as Lake Constance, the concentrations of alkalinity and Ca in the top layer (0 to 50 m) only indicated an upward tendency (Barbier et al. 2017), estimated from lake data retrieved from https://si-ola.inra.fr. The reason for the different result could be that the re-oligotrophication process has not proceeded as far as in Lake Constance. In fact, the concentration of dissolved reactive phosphorous in Lake Geneva has not yet come down to the natural level of a few micrograms as in Lake Constance, after the pollution induced peak of about 80 μg P L^{-1} in the early 1980s in both lakes https://www.bafu.admin.ch/bafu/de/home/zustand/indikatoren.html.

3. The decreases in the strong acid inputs into the subsurface, as a result of the diminishing use of N fertilizer and the decreasing atmospheric deposition, lowered the quantity of acids available to weather calcite and dolomite. Consequently, the amount of alkalinity, Ca, and Mg produced was decreasing.

In rivers with no lakes upstream, the balance between driver 1 and driver 3 regulates the changes in alkalinity, Ca, and Mg. In the alpine rivers Rhine and Rhone, at stations DI and PO, the "alkalinity increasing" driver 1 is dominating. The reverse holds in the Thur at station AN, where driver 3 is dominant.

At the Rhine stations RE and VW, situated downstream of Lake Constance and Lake Geneva, the two "alkalinity increasing" drivers outbalance the "alkalinity diminishing" driver. The changes reported at the Rhône station CH and at the Aar station BR (Tables 2 and 4) do not provide a clear conclusion with respect to these drivers. Concentrations of alkalinity were increasing, but that of Ca did not change significantly at station CH, but decreased clearly at station BR.

CO_2 outgassing from rivers

The positive difference between the concentrations of "native H_2CO_3" and H_2CO_3 determined in the rivers indicates a clear outgassing of CO_2 over the flow path of the water from the location of initial carbonate dissolution to the measuring station. This difference includes CO_2 generated by the biogeochemical processes on the flow path of water, such as the degradation of allochthonous and autochthonous organic carbon (not known quantitatively), the acid produced by nitrification of ammonium, and the part of CO_2 formed by the precipitation of calcite in lakes. Estimated annual fluxes per catchment area of CO_2 outgassing varied greatly from 268 mmol m^{-2} a^{-1} at station AN with no lakes in the catchment to 3 mmol m^{-2} a^{-1} at station CH situated downstream of the large Lake Geneva (Table 4 (c)). The negative flux at station PO reflects a special situation of this alpine catchment. Here, calculated "native H_2CO_3" (Table 4) indicated an undersaturation with respect to H_2CO_3 in river water, which might be due to a large portion of surface runoff originating from snow and ice melting. Consequently, water will absorb CO_2 on the flow path and the H_2CO_3 concentration increases. Under this condition, the calcite in river water at station PO was more or less equilibrated (Table 4). This result is in contrast to the distinct oversaturation at the other stations.

In the literature, a diffusion model is usually implemented to estimate the flux of outgassing (evasion) CO_2. In this model, the flux is calculated as the difference between partial pressure of CO_2 (pCO_2) in the river (calculated with measured pH and water composition) and the atmospheric pCO_2 multiplied by a not univocal gas transfer velocity of CO_2 (Raymond et al. 2012; Geldern et al. 2015 and many others). Flux obtained per area of surface water is converted to flux per area of the catchment by estimating the water to catchment area ratio; see, for example, Geldern et al. (2015). These authors applied the diffusion model in a Bavarian river situated in a catchment of 1040 km^2, about 300 km northeast of Switzerland, and exhibiting a carbonate lithology. They reported a median CO_2 evasion rate of 145 mmol m^{-2} a^{-1} calculated over the catchment area. In this case study, evasion rates per river area fell by a factor of 25 from the source to the outlet station. For comparison, the mean global CO_2 evasion rate estimated by Lauerwald et al. (2015) amounts to 410 mmol m^{-2} a^{-1}, assuming a land surface area of 132×10^6 km^2. Application of the diffusion flux method to our rivers, using a gas transfer coefficient K of 6.3 m day^{-1}, resulted in a CO_2 transfer per catchment area in the range from 34 to 306 mmol m^{-2} a^{-1} (Table 4 (c)).

It is interesting to note that some values of the two approaches (Δ concentration, diffusion) were in a similar range, although they were based on different models. To make this difference more clearly understandable, our proposed method (Δ concentration) to quantify CO_2 outgassing estimates the gas transfer over the flow path from the origin to a measuring station, while the diffusion model estimates the quantity of CO_2 that could be transferred from the water at the station to the atmosphere. A thorough discussion of this discrepancy between the two models goes beyond this work.

Ratio of Ca to Mg concentration

The ratio of Ca to Mg reflects the relationship between calcite and dolomite weathering (Szramek et al. 2011). A molar ratio Ca_{corr}/Mg of 2.84 corresponds to a calcite to dolomite mass ratio of 1:1. In the alpine rivers Rhine and Rhône at station DI and PO, the molar ratios were lower than 2.84 (Suppl.Table 4) and indicate the prevalence of weathered dolomite over calcite.

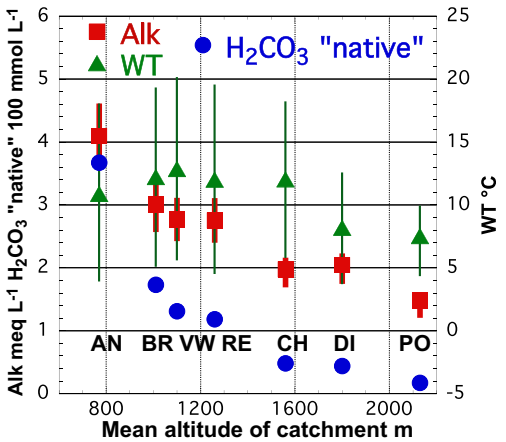

Fig. 5 Multiannual means of alkalinity (Alk), water temperature (WT), and "native H_2CO_3" in the period from 2009 to 2013 in relation to the mean altitude of the catchment. Bars indicate the mean seasonal fluctuations. Those of "native H_2CO_3" are too small to be visible. For abbreviations of stations, see Table 1

At the stations VW, RE and BR molar ratios were higher than 2.84; they express the dominance of calcite weathering. The significant decreases in the molar ratios of Ca_{corr}/Mg and of alkalinity/Mg and the increase in the ratios of alkalinity/Ca_{corr} (Table 4 Supp Info) at stations VW, RE, BR, and CH, which are situated downstream of lakes, indicated an increasing tendency for calcite precipitation in rivers and connected lakes (Szramek et al. 2011). The river Thur did not indicate such a reaction, although the estimated outgassing rate was high. In the alpine Rhine at station DI, the change in the three ratios reversed, pointing to an increasing dissolution of calcite with time.

Effect of altitude on alkalinity, water temperature and "native H_2CO_3" concentration

The negative relationships between concentrations of alkalinity, water temperature, "native H_2CO_3," and mean altitude of the catchment (Fig. 5) clearly infer the effect of the altitude on alkalinity, water temperature, and calculated "native H_2CO_3." Alkalinity decreased by 0.17 meq L^{-1} per 100 m (Suppl. Fig. 4), water temperature declined by 0.33 °C per 100 m, and "native H_2CO_3" decreased exponentially. As displayed in Suppl. Fig. 4, Ca minus SO_4 (Ca_{corr}) decreased synchronously with alkalinity, indicating a very similar dependency in the weathering of calcite and dolomite with altitude. The small fractions of crystalline lithology present in the catchments only induce a small effect on the concentration ranges of alkalinity in the altitude profile. At higher-altitude sparse vegetation, thin soils and low temperatures result in a low microbial activity in the subsurface. Consequently, less CO_2 is produced to weather rock minerals. Calmels et al. (2014) have found that in the calcareous Jura Mountains bordering Switzerland, the change in the type of vegetation from deciduous to coniferous with altitude also plays an important role in the gradient of CO_2. Lauerwald et al. (2013) and others also reported higher alkalinity concentrations in catchments with a higher proportion of agricultural land and of carbonate lithology. In our study, the latter factor only plays a minor role since all catchments are dominated by calcareous rock. The River Thur exhibited by far the highest alkalinity, reflecting a Swiss lowland catchment with a high percentage of agricultural land and the dominance of carbonates in the underlying bedrock. Figure 5 also demonstrates that seasonal fluctuations of alkalinity were often smaller than the differences between means of stations, whereas water temperatures exhibited the reverse relation.

Chemical weathering rates

The chemical weathering rates of the rock-forming minerals can be estimated stoichiometrically by apportioning measured loads (corrected for atmospheric deposition) to the individual weathering reactions (Suppl. Table 3). Drever (1997) discusses this allocation procedure in detail. Previous results for some of the rivers studied were documented (Zobrist 2010).

In the Rhine at station DI, no statistically significant changes in the loads of the geochemical parameters can be detected, and therefore no changes in the weathering rates of calcite, dolomite, and silicates could be deduced for this alpine catchment. Also in the Thur, a river with no lakes in the catchment, no significant changes in loads were found. In the river Rhône at station PO, only H_4SiO_4 loads showed a significant decrease of 10%. The results imply that at these three stations, the observed increase in the concentrations of total hardness, alkalinity, Ca, and Mg do not alter the overall chemical weathering rates of carbonate rocks to a statistically significant degree. Only at station CH did the loads of all geochemical species decrease due to the significant decrease in water discharge (13%), which overcompensates for the increase in concentrations.

In the allocation procedure for the chemical weathering of gypsum/anhydrite, changes in the atmospheric sulfur deposition also play a role. At the stations AN, BR, and VW, the means of the significant decreases in SO_4 areal loads correspond approximately to the decrease in the atmospheric sulfur deposition by 39 mmol m^{-2} a^{-1} during the study period. At stations CH, PO, and DI, these changes were below the precision of the SO_4 areal loads > 450 mmol m^{-2} a^{-1}. This would suggest that the weathering rates of gypsum/anhydrite did not change. The documented increases in water temperature would increase the solubility of the gypsum by less than 1%, which is smaller than the precision of the SO_4 loads. Therefore, the observed temperature increases cannot provoke a detectable increase in the weathering rate of gypsum/anhydrite.

The weathering reconstruction procedure allows an estimation of the different sources of alkalinity. The weathering of silicate minerals by CO_2 and H^+ also produces alkalinity (Suppl. Table 3). Although incongruent dissolution reactions of silicates vary greatly (Drever and Zobrist 1992), it can be assumed that per 1 mol of H_4SiO_4, approximately one equivalent of alkalinity and one equivalent of the base cation sum (Ca, Mg, Na, K) are released. The allocation calculations documented that only a few percent (1.5 to 3.5%) of the alkalinity and of the base cation Ca, Mg, and Na originate from the weathering of silicates. In contrast, the weathering of silicates in alpine catchments can contribute noticeably to dissolved K. In catchments exhibiting a distinct percentage of agricultural land (Table 1), K also derives from fertilizer use. Calculations further indicated that the acid deposition and nitrification of N_{red} produced about 5 to 6% of the alkalinity. Still smaller was the contribution of the acid produced by the oxidation of sulfide-containing minerals, mainly pyrite, due to the small pyrite content in calcareous rocks (0.1 to 0.4%). Therefore, the weathering of calcareous minerals by CO_2 produced more than 90% of the alkalinity measured. Areal loads of alkalinity varied between stations from 1.5 to 3.5 mol m^{-2} a^{-1}. The long-term means of 2.55 mol m^{-2} a^{-1} at the Rhine border station VW and 2.1 mol m^{-2} a^{-1} at the Rhone

border station CH distinctly exceed the European averages of 0.35 mol m^{-2} a^{-1}, but they are higher than those in the Slovenian Sava catchment (Szramek et al. 2011).

According to the weathering reaction of carbonates, half of the alkalinity produced originates from the subsurface H_2CO_3. Therefore, in the catchments of the Rhine and Rhône, the weathering of rocks sequesters 1.2 and 1.0 mol m^{-2} a^{-1} of atmospheric CO_2. Comparisons with the quantity of CO_2 outgassed (Table 4 (c)) disclose that a few percent (Thur 15%) are released to the atmosphere again on the flow path of the river, as discussed before. A similar percentage of CO_2 loss can be estimated from the data of Geldern et al. (2015) measured in the Bavarian river.

Mineral equilibrium and dynamics of H_4SiO_4

The equilibrium calculation using Visual MINTEQ expressed a minor undersaturation of measured H_4SiO_4 concentration with respect to quartz (Table 4). As pH and water temperature increased, the undersaturation of quartz slightly decreased. Rather than referring to equilibria with crystalline rock minerals (Drever and Zobrist 1992), we think that our data set of silicic acid indicates interesting aspects that have no yet sufficiently been recognized in literature.

The weathering of silicate minerals in catchments without lakes (indicated at stations DI, PO, and AN) produced mean concentrations of H_4SiO_4 in waters in the range of 0.05 to 0.065 mmol L^{-1} (Fig. 3). The time series of the trend component showed significant negative changes (Table 2). In contrast, time series at stations downstream of lakes, RE, VW, BR, and especially CH displayed lower concentration ranges and positive linear trends, except at station CH where it is negative.

Lakes act as sink for H_4SiO_4 due to the use of H_4SiO_4 by diatoms to build up their skeleton. As diatoms sink and settle, a fraction of Si is buried in the sediments (Wessels et al. 1999). The distinct smaller mean concentration of H_4SiO_4 of 0.026 mmol L^{-1} at the outflow of Lake Geneva (station CH), compared to the main inflow (station PO) with a mean of 0.053 mmol L^{-1}, illustrates the elimination effect for H_4SiO_4 by the precipitation of diatoms. During the re-oligotrophication phase, the abundance and taxonomic composition of diatoms changed; specifically, the abundance of sedimenting species declined (Rimet 2009, p. 80; igbk 2014; Bürgi 2015). As a consequence, the overall concentration of H_4SiO_4 in the lake increased. Concerning our study, the H_4SiO_4 concentration in the top layer (0 to 5 m) of the Lower Lake Constance (Untersee, the Western arm of the lake) increased by 0.3 μmol L^{-1} a^{-1} from 1996 to 2013 (H. Ehmann, State Water Protection State Thurgau, personal communication, December 2015). This rise is consistent with an increase of 0.36 μmol L^{-1} a^{-1} at the downstream station, RE (Table 2). In Lake Geneva, the H_4SiO_4 concentration in the top layer (0 to 50 m) decreased by 0.12 μmol L^{-1} a^{-1} from 1983 to 2013. Also consistently, the downstream station CH exhibited a linear decrease of 0.19 μmol L^{-1} a^{-1} (Barbier et al. 2017), and data for calculation was retrieved from https://si-ola.inra.fr. This difference in decreasing rates between the two large lakes may be due to the lower eutrophic state of Lake Constance than that of Lake Geneva, reflected by the presently lower concentration of dissolved reactive phosphorous in Lake Constance of 6 μg L^{-1} compared to 20 μg L^{-1} in Lake Geneva (igbk 2014; CIPEL 2017).

Potassium, sodium, and chloride

Annual means of K concentrations varied from 0.02 to 0.03 meq L^{-1} in the alpine river at station DI and from 0.06 to 0.08 meq L^{-1} in the Thur. Standardized 5-year STL trends (Suppl. Fig. 5) showed steps in time evolution which were due to modifications in analytical methods (Report in Suppl. Material). They render interpretation of long-term changes questionable for K but not for Na.

The average concentrations for Na and Cl ranged from 0.1 to 0.4 mmol L^{-1}. The highest concentrations observed in all rivers studied amounted to 1.4 mmol L^{-1} in the Thur. It had been measured in the biweekly sample after a longer freezing period. This maximal concentration is similar to that measured during the winter in the Mohawk River, NY, USA (Godwin et al. 2003), in a sparsely populated catchment. Cl and Na concentrations in the range of a few millimoles per liter did not yet show deteriorating effects on the ecology (Factsheet, FAQ use of deicing products in Switzerland; http://www.eawag.ch/fileadmin/Domain1/Beratung/Beratung_Wissenstransfer/Publ_Praxis/Faktenblaetter/fb_Streusalz_Nov2011.pdf) (Ramakrishna and Viraraghavan 2005). This assessment stands in contrast to much higher values, up to

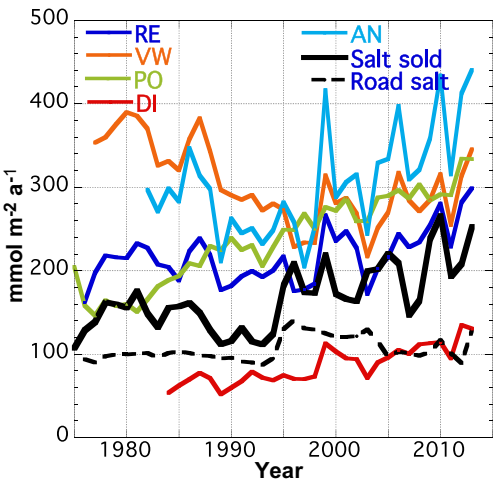

Fig. 6 Long-term changes in the annual Cl areal loads in selected rivers and in the annual sale of salt (NaCl) and road salt (de-icing salt) in Switzerland. Omitted stations BR and CH display time courses and ranges similar to those at stations PO and RE. Units are standardized to the area of the catchments and of the country. For station abbreviations, see Table 1

130 meq L^{-1}, measured in US urban streams during winter, marking the effect of concentrated deicing salts inputs (e.g., Kaushal et al. 2005; Novotny et al. 2009).

In the rivers studied, the Na concentrations surpassed those of Cl by 0.01 to 0.04 mmol L^{-1}. The weathering of siliceous minerals contributed approximately 0.015 mmol L^{-1} to the excess of Na in alpine rivers. The reminder originated from other sources, such as ion exchange with Ca in soils or the discharge of industrial wastewater. The concentration ranges observed and the distinct increases of the Cl concentration from 2.1 to 4.4 μmol L^{-1} a^{-1} (Table 2) clearly reflect the anthropogenic input of NaCl salt. The salt produced by the Swiss salt refineries increased from 360 kt NaCl a^{-1} in the 1980s to presently up to 560 kt NaCl a^{-1}, corresponding to 70 kg a^{-1} and capita or 232 mmol a^{-1} per m^{-2}. This represents approximately the total salt use in the whole country. The mean of deicing salt sold, almost all NaCl, amounted to 128 mmol m^{-2} a^{-1} or to 38 kg NaCl a^{-1} and capita in the last 5 years. However, salt use varies from year to year (http://www.salz.ch/de/downloads). As would be expected, the quantity of road salt applied, displayed in Fig. 6, depends primarily on the air temperature, the snowfall regime in winter, and the length of the road networks in a catchment. Also notable, improved spreading techniques have lowered the applied quantity of salt per surface area of road, but the overall use of salt has nevertheless increased.

The time course shown in Fig. 6 for the annual areal loads of Cl and for salt sold indicated a clear increase (except at station VW). At this station, the diminishing areal load of Cl, as well as the decreasing concentrations up to 2000, was due to a change in production schemes at the numerous chemical plants situated along the Swiss-German border of the Rhine (Hochrhein). In Fig. 6, the significant linear slopes of areal loads in rivers ranged between 2.3 and 4.3 mmol m^{-2} a^{-1}. Those of total salt and road salt exhibited similar rates, respectively 3.6 and 3.0 mmol m^{-2} a^{-1}. From 1983 to 2013, annual Cl loads in rivers increased on the average by 60% (station BR 9%, station Di 125%). During this period, the total salt produced and used increased by 53% and that of deicing salt increased by 148%, while the population grew only by 23%. The areal loads of Cl correlated significantly and positively with yearly sales of NaCl (except at stations VW and BR), indicating the driving forces for the increasing concentrations and loads observed. Yearly peaks and troughs in areal loads coincided only sometimes with salt sold, as the sale and the year of application may be different, especially in the case of deicing salt. In addition, a notable part of the deicing salt applied remains transiently in soils, groundwater, and lakes (Kelly et al. 2008; Novotny et al. 2009). In the catchment of Lake Constance, the remaining part of salt used made up to 35% of a yearly input (Mueller and Gaechter 2012). This retardation of Cl and the deferred application of deicing salt related to the period of sales resulted in an uncertain correlation between yearly sale of deicing salt and yearly loads in rivers.

The alpine catchment of the Rhine (station DI) and Rhône (station PO) exhibited quite different results in areal loads and loads per capita. At station DI, the areal load of 118 mmol m^{-2} a^{-1} (mean 2009 to 2013) fell distinctly below those of the other catchments, except the Thur (230 to 303 mmol m^{-2} a^{-1}), while the load per capita remained in the range of the other stations (45 to 61 kg a^{-1} and capita). At station PO, the areal load of 307 mmol m^{-2} a^{-1} was in the range of the others stations, whereas the load per capita was three times higher. This comparison indicates additional sources of Cl beside road salt in the Rhône catchment at station PO. There exist two additional sources with unknown outputs: (1) The catchment exhibits evaporate rocks containing halite which are a source of Cl. (2) The chemical industries in the Rhône valley use large amounts of chlorine (Cl_2) for organic synthesis, presently in the range of 20,000 t per year, corresponding to 65 kg per capita or 54 mmol m^{-2} a^{-1}. A part of this chlorine is reduced to chloride and reaches the river with wastewater. As displayed in Suppl. Material, Report (last Figure), the small seasonal variation of Cl loads suggests an important contribution of the last two sources mentioned. For comparison, the estimations (Zobrist and Reichert 2006) for the partitioning of the measured Cl areal loads into diffuse and point sources in Switzerland gave a value of 30 mmol m^{-2} a^{-1} for the natural background, 245 mmol m^{-2} a^{-1} for intensively used agricultural land, and 30 kg per capita (settlement and traffic areas included). The calculated sum of these export coefficients times the corresponding area/population for the Rhône catchment only made up half of the measured loads at stations PO and CH. This result provides another evidence for the existence of additional Cl sources in this catchment.

Nitrogen

The time series of the 5-year STL trend components for concentrations and loads of NO_3 and total N (Fig. 7) have the following characteristics in common: (1) the distinct and concurrent increase in NO_3 and total N concentrations and loads around 1986; (2) the decrease in differences between total N and NO_3 after 1990; (3) the 95% confidence intervals for the loads which were greater than those for concentrations; and (4) a similar pattern of fluctuation of standardized trend components which is shown in Suppl. Fig. 6.

For NO_3, the STARS test indicated a significant upward shift in concentrations in the range of 240 to 480 μg N L^{-1} in non-alpine rivers and of 60 μg N L^{-1} in the alpine Rhône, all occurring in the period between 1984 and 1987 (Suppl. Table 2). Upward shifts in NO_3 loads also occurred in the same period, but the relative increases were smaller than those estimated for concentrations. The 5-year STL trend components of total N concentrations highlighted a similar evolution at all stations, with an increase in the period from 1984 to 1986, followed by a decrease until around 2005 and almost no change from 2006 to 2013. In the first period, the STARS

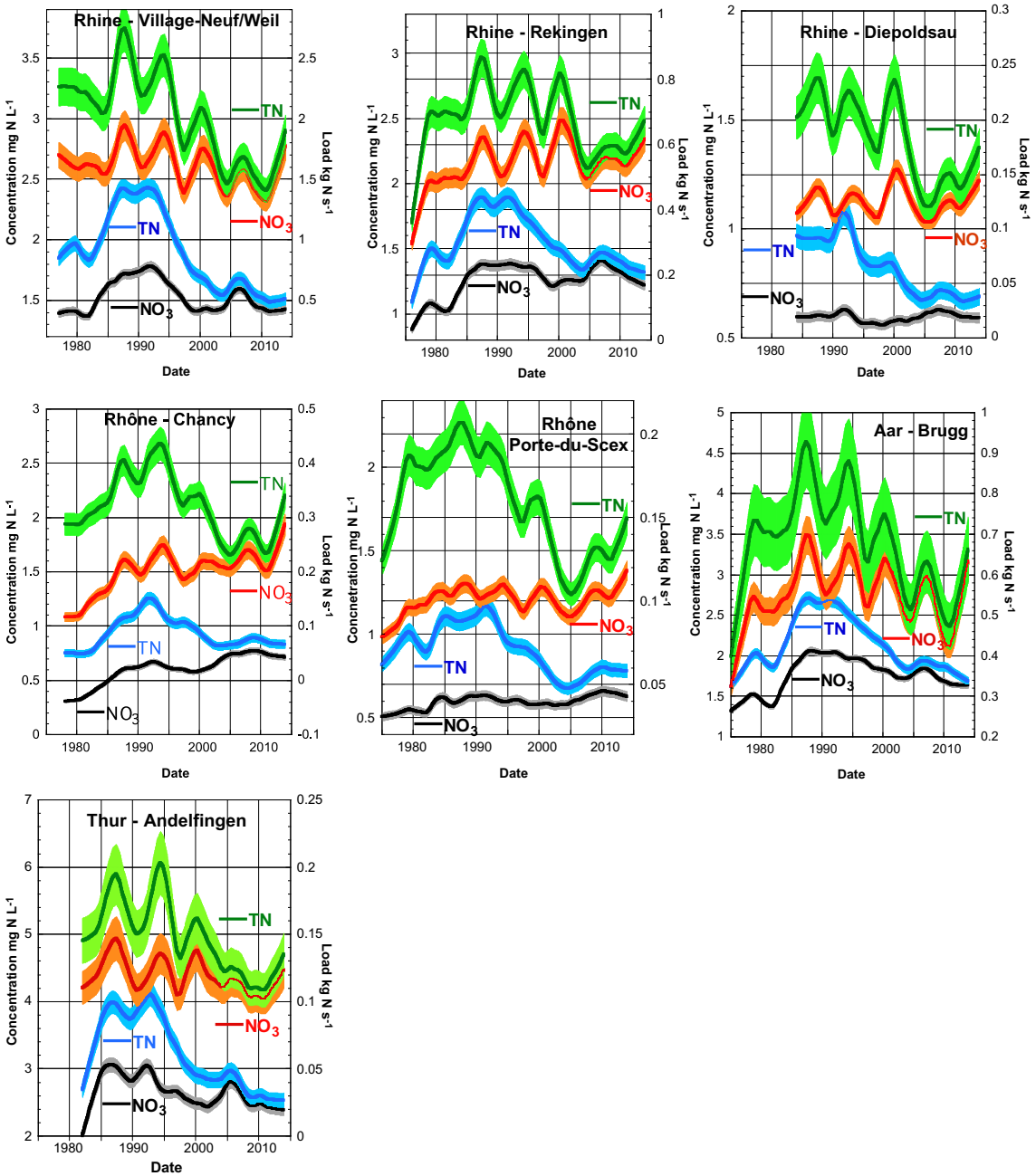

Fig. 7 Time series of 5-year STL trend components for concentrations and loads of nitrate (NO_3) and total nitrogen (TN). Lower curves (black and blue) are concentrations, and upper curves (red and green) are loads. Shaded areas represent 95% confidence interval. The x-axis labels refer to the first day of the year

tests indicated significant upward shifts in concentrations ranging from 180 to 690 μg N L^{-1}, representing 10 to 30% of the means preceding the shifts. In the period from 1994 to 1999, downward shifts ranged from 240 to 920 μg N L^{-1} (21 to 31% of preceding means). For loads of total N, the upward shifts occurred in the same period as for concentrations, but the years of downward shifts varied between stations (Suppl. Table 2). At all stations, concentrations and loads of total N decreased distinctly over the period between 1983 and 2013, whereas those of NO_3 changed less and varied in sign and between stations (Tables 2 and 3). As discussed, concentrations and loads of N species show a characteristic evolution and larger changes than the geochemical parameters. This fact stimulates a discussion about possible causes for these changes.

In the following, we first present a hypothesis to explain the common increases of the total N concentrations and loads in the late 1980s and the decreases in the following years, as

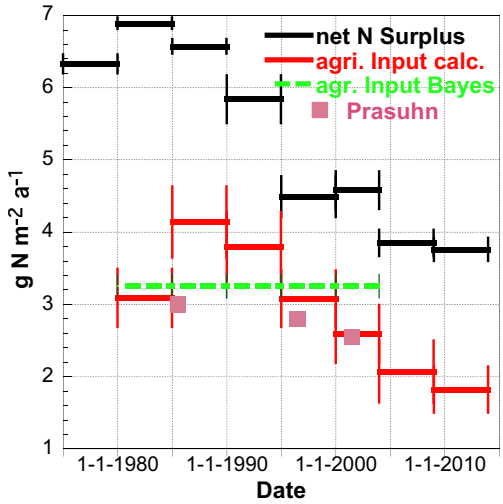

Fig. 8 Comparison of four different methods to estimate the diffuse input of total nitrogen (TN) by intensively used agricultural land. **a** Stepwise evolution of the 5-year means of the areal agricultural net surplus of nitrogen. **b** Stepwise evolution of the 5-year means of the diffuse river agricultural input calculated from measured data. Mean of four catchments (VW, RE, BR, AN) exhibiting more than 29% fertilized land. **c** Estimation by Bayes regression from 1980 to 2003 (Zobrist 2006, p. 18). **d** Estimation by the MODIFFUS regional emission model of Prasuhn (2005, p. 54). (Agricultural net surplus of N-net agricultural input of N minus the emission of N to the atmosphere. Diffuse river input from agriculture: measured load of TN minus wastewater input minus natural diffuse inputs. For a detailed explanation, see Suppl. Table 6). Vertical bars indicate standard deviations **a** of the means in the 5-year period, **b** of the four stations, and **c** of regression

displayed in Fig. 7 and more specifically in Suppl. Figs. 1 and 6. We then discuss the reasons for the observed changes by providing estimates for the changes of the N input from agricultural intensively used land.

We hypothesize that two simultaneous processes may explain the notable increase in loads, as well as in concentrations of N in the period from 1982 to 1987: (1) The increase in the input of the pollution source "agricultural net surplus of total N" (for a definition, see Suppl. Table 6) provoked a delayed increase of total N discharged into waters in the early 1980s. (2) The distinct increase in water and soil temperatures in the period from 1986 to 1989 (Fig. 2a) accelerated the biological activities in soils and consequently caused a temporarily higher discharge of N from agricultural and natural sources, as was also observed by Rogara (2007). The input from natural sources represents only a minor fraction of the total N loads in the non-alpine rivers (Zobrist and Reichert 2006); therefore, their potential change by the previously discussed temperature shift will be small and can be ignored.

In order to identify the reason for the increasing and decreasing time course of total N loads displayed in Fig. 7, we compare two different approaches to estimate the N input to rivers by agriculture from intensively used land (Fig. 8): In the first approach, the net agricultural surplus of N is estimated based on the model and data cited in Suppl. Table 6. It is reported as load per area of agricultural land. In the second approach, the agricultural input is estimated from measured loads in rivers minus inputs for the known other sources of N (wastewater and natural diffuse sources). It is reported as load per area of catchment. As the considered areas in the two approaches are not the same, the numeric values obtained must be different. Now, we assume that the evolution in time of the two estimates will be similar if the changes in the net agricultural surplus of N is the main cause for the observed changes in the total N loads in rivers. In fact, in Fig. 8, a similar pattern in the stepwise evolution in areal loads of the net agricultural surplus and that of the load from intensively used agricultural land (mean of the four stations in the Rhine catchment downstream lakes) is observed. It indicated that the upward shift in the late 1980s and the following decrease in riverine loads, displayed in Fig. 7 and Suppl. Fig. 6, could be explained by the changes in the net agricultural N surplus. The small time lag between the two curves reflects the retarded increases of N in the rivers, due the slow elution process of N from soil. Also notably, the calculated values for the areal agricultural load displayed in Fig. 8 corresponded reasonably well to the reported values, obtained by the MODIFFUS regional emission model for the Swiss part of the Rhine catchment downstream of lakes (Prasuhn and Sieber 2005) or to the export coefficient from intensively used agricultural land by Bayes regression in the period 1980–2003 (Zobrist and Reichert 2006). If the load for wastewater inputs, due to the application of the denitrification process in some treatment plants, could reduce the input by 10% in approach 2, the calculated input from agricultural intensively used land would increase by 0.15 g N m^{-2} a^{-1}. This correction could lessen the difference between the net N surplus and the agricultural areal load in the last two 5-year periods, in which the introduction of the denitrification process in the treatment plant was initiated. In conclusion, these considerations, although tentative, are based on an extensive amount of information and can semi-qualitatively explain the observed time course of the measured total N loads in rivers. The result also indicates that pollution-preventing measures taken in agricultural practices, as well as in wastewater treatment, have successfully decreased the pollution load of N. In Germany, such prevention measures resulted in a distinct decline of the nutrient inputs of N and P to surface from the 1980s to the present (https://www.umweltbundesamt.de/daten/wasser/fliessgewaesser/eintraege-von-naehr-schadstoffen-in-die).

The different decreases in concentrations and loads of total N (mainly ammonium and organic N) and NO_3 (Fig. 7) over time can be explained qualitatively by the different changes in the input of NO_3 by wastewater treatment plants. The improvement in treatment by nitrification has lowered the input of ammonium and increased that of NO_3, but did not decrease that of total N substantially. Although no data is available, we can assume that the NO_3 input by agricultural sources has also

decreased. Depending on the relationship of these two inputs from wastewater and agricultural land over time, measured loads of NO_3 at a station can decrease, increase, or exhibit no change at all (Table 3). This implies that the evolution of the overall loads for NO_3 and for total N loads in rivers with time does not proceed concurrently, as is often argued in the discussion of pollution prevention measures.

Conclusions

The statistical methods applied to the long-term time series of physical parameters, concentrations, and loads of chemical constituents made the following possible:

- -To determine the long-term changes in measured data by eliminating the seasonal variations (by STL) and to compare rivers by standardized time series
- -To estimate monotonic trends from 1983 to 2013 using linear regression analysis
- -To detect and quantify discontinuities in time series (by STARS)

A detailed consideration of catchment characteristics, geochemical processes, and quantitative data on environmental factors and on human activities enabled us to determine the drivers and the causes/factors responsible for the observed changes in concentrations and loads in rivers.

The identified trends of geochemical and N species indicated various effects that can be ascribed to global warming and to consequences of measures taken to reduce pollution.

The rivers studied present a "high water discharge" system ($\pm$ 1 m a^{-1}), and they can be regarded as less impacted anthropogenically in comparison to major "low water discharge" rivers in other industrialized and/or agricultural regions, such as the Mississippi (0.2 m a^{-1}) or the Thames (0.16 m a^{-1}). As a consequence, drivers identified in this study do not necessarily have to agree with those assigned in the large "low water discharge" catchments. However, the results obtained in this study contribute a new and important component to the knowledge of different environmental river systems.

The results obtained via extended data evaluation validate the benefit and relevance of this long-term monitoring program based on continuous water-discharge proportional samples. This special sampling system and the data record make it possible to detect small changes in water quality and fluxes altering geochemical processes and ecological systems. This is highly relevant in the national as well as in the global context of warming effects in alpine regions. It merits the continuation of the NADUF program and may support the continuation or start of similar program elsewhere, at least with a few benchmark stations for a large river system (Burt et al. 2010).

Acknowledgments We gratefully acknowledge the constant effort of numerous collaborators at the "Federal Hydrological Survey" (official name changed many times), at the analytical laboratory and in the data-handling group at Eawag, who have reliably and continuously carried out the long-term river survey NADUF for more than 40 years. We also thank David Livingstone, Rolf Kipfer, and Laura Sigg for their valuable comments and support. The suggestion and comments of two anonymous reviewers are also highly appreciated. Lastly, we are grateful to Jay Matta for improving the English writing.

References

Ahel M, Molnar E, Ibric S, Giger W (2000) Estrogenic metabolites of alkylphenol polyethoxylates in secondary sewage effluents and rivers. Water Sci Technol 42:15–22

Arona R, Tockner K, Venerohr M (2016) Changing river temperatures in northern Germany: trends and drivers of change. Hydrol Process 30: 3084–3098

Barbier C, Quetin P, Anneville O (2017) Evolution pyhisco-chemique des eaux du Léman et données météoroloquiques, Commision internationale pour la protection des eaux du Léman contre la pollution. CIPEL, Nyon

Berge E, Bartnicki J, Olendrzynski K (1999) Long-term trends in emissions and transboundary transport of acidifying air pollution in Europe. J Environ Manag 57:31–50

Bundi U, Peter A, Frutiger A, Huette M, Liechti P, Sieber U (2000a) Scientific base and modular concept for comprehensive assessment of streams in Switzerland. Hydrobiologia 422(423):477–487

Bundi U, Peter A, Truffer B, Wagner W, Mauch U, Scheidegger A (2000b) The quality of aquatic ecosystems as an indicator for sustainable water management - country paper of Switzerland. In: Kraals JA (ed) Let the fish speak: the quality of aquatic ecosystems as an indicator for sustainable water management. EurAqua technical review. Institute for Inland Water Management and Waste Water Treatment, Lelystad, pp 205–215

Bürgi HR (2015) 50 Jahre Planktonentwicklung im Vierwaldstättersee von 1960 bis 2010. Aufsichtskommission Vierwaldstättersee (AKW), Stans

Burt TP, Howden NJK, Worrall F, Whelan MJ (2010) Long-trem monitoring of river water nitrate: how much data do we need? J Environ Monit 12:71–79

Calmels D, Gaillardet J, Francois L (2014) Sensitivity of carbonate weathering to soil CO2 production by biological activity along a temperate climate transect. Chem Geol 390:74–86

CIPEL (2017) Rapports sur les études et recherches entreprises dans le bassin lémanique (in french). Interational commitee for the Protection of the Water of Lake Geneva. CIPEL, Nyon

Cleveland RB, Cleveland WS, McRae JE, Terpenning I (1990) STL: a seasonal-trend decomposition procedure based on Loess. J Off Stat 6:3–73

Drever JI (1997): The geochemistry of natural waters: surface and groundwater environments, 3rd ed. Prentice Hall, Upper Saddle River, NJ 07458, pp. 436

Drever JI, Zobrist J (1992) Chemical weathering of silicate rocks as a function of elevation in the Southern Swiss Alps. Geochim Cosmochim Acta 56:3209–3216

Esterby SA (1996) Review of methods for the detection and estimation of trends with emphasis on water quality applications. Hydol Process 10:127–149

Federal Office for the Environment F 2015: NABEL Luftbelastung 2014, Federal Office for the Environment (Foen), Swiss Federal Laboratories for Material Sciences and Technology (Empa)

Figura S, Livingstone DM, Hoehn E, Kipfer R (2011) Regime shift in groundwater temperature trigger by the Artic Ocillation. Geophys Res Lett 38

Friedman JH, Stuetzle W (1981) Projection pursuit regression. J Am Stat Assoc 76:817–823

Geldern Rv SP, Mader M, Baier A, Barth JAC (2015) Spatial and temporal variations of pCO2, dissolved inorganic carbon and stable isotopes along a temperate karstic watercourse. Hydrol Process 29: 3423–3440

Giger W, Schaffner C, Kohler HPE (2006) Benzotriazole and tolyltriazole as aquatic contaminents. 1. Input and occurrences in rivers and lakes. Environ Sci Technol 40:7186–7192

Gnägi C, Labhart TP (2017) Geologie der Schweiz. Ott Verlag, Bern

Godwin KS, Hafner SD, Buff MF (2003) Long-term trends in sodium and chloride in the Mohawk River, New York: the effect of fifty years of road-salt application. Environ Pollut 124:273–281

Hirsch RM (2014) Large biases in regression-based constituent flux estimates: causes and diagnostic tools. J Am Water Resour Assoc 50: 1401–1424

Hirsch RM, Alley WM, Wilber WG (1988): Concepts for a national water-quality assessment program (NAWQA). U.S. Geological Survey

Hirsch RB, Alexander RB, Smith RA (1991) Selection of methods for the detection and estimation of trends in water quality. Water Resour Res 27:803–813

Hirsch RB, Hamilton PA, Miller TL (2006) U.S. Geological Survey perspective on water-quality monitoring and assessment. J Environ Monit 8:512–518

Howden NJK, Burt TP, Worrall F, Whelan MJ, Bieroza M (2010) Nitrate concentrations and fluxes in the River Thames over 140 years (1868–2008): are increases irreversible? Hydrol Process 24:2657–2662

igbk (2014) Yearly Report Nr. 40, Limnologischer Zustand des Bodensees (in German). International Commission fort he Protection of Lake Constance. Institut für Seenforschung,- D-88081 Langenargen

Jakob A, Binderheim-Bankay E, Davis JS (2002) National long-term surveillance of Swiss rivers. Verh Internat Verein Limnol 28:1101–1106

Kaushal SS, Groffman PM, Likens GE, Belt KT, Stack WP, Kelly VR, Band LE, Fisher GT (2005) Increased salinization of fresh water in the northeastern United States. Proceed Nat Acad Sci United States 102:13517–13520

Kaushal SS, Likens GE, Jaworski NA, Pace ML, Sides AM, Seekell D, Belt KT, Secor DH, Wingate RL (2010) Rising stream and river temperatures in the United States. Front Ecol Environ 8:461–466

Kaushal SS, Likens GE, Utz RM, Pace ML, Grese M, Yepsen M (2013) Increased river alkalinization in the Eastern U.S. Environ Sci Technol 47

Kelly VR, Lovett GM, Weathers KC, Findlay SEG, Strayer DL, Burns DJ, Likens GE (2008) Long-term sodium chloride retention in a rural watershed: legacy effects of road salt on streamwater concentration. Envriron Sci Technol 42:410–415

Lauerwald R, Hartmann J, Moosdorf N, Kempe S, Raymond PA (2013) What controls the spatial patterns of the riverine carbonate system?—a case study for North America. Chem Geol 337-338:114–127

Lauerwald R, Laruelle GG, Hartmann J, Ciais P, Regnier PAG (2015) Spatial patterns in CO2 evasion from the global river network. Glob Biogeochem Cycles 29:534–554

Macpherson GL, Roberts JA, Blair JM, Towsend MA, Fowle DA, Beisner KR (2008) Increasing shallow groundwater CO2 and limestone weathering Konza Prairie, USA. Geochim Cosmochim Acta 82:5581–5599

Moser A, Wemysss D, Scheidegger R, Fenicia F, Honti M, Stamm C (2017) Modelling biocide and herbicide concentrations in catchments of the Rhine basin. Hydrol Earth Syst Sci Discuss. under review

Mostert E (2009) International co-operation on Rhine-water quality 1945-2008: an example to follow? Phys Chem Earth 34:142–149

Mueller B, Gaechter R (2012) Increasing chloride concentrations in Lake Constance: characterization of sources and estimation of loads. Aquat Sci 74:101–112

Mueller B, Meyer JS, Gaechter R (2015) Alkalinity regulation in calcium carbonate-buffered lakes. Limnol Oceanogr 61:341–352

North RP, Livingstone DM, Hari RE, Köster O, Niederhauser P, Kipfer R (2013) The physical impact of the late 1980s climate shift on Swiss rivers and lakes. Inland Waters 3:341–350

Novotny EV, Sander AR, Mohseni O, Stefan HG (2009) Chloride ion transport and mass balance in a metropolitan area using road salt. Water Resour Res 45:W12410

Orr HG, Simpson GL, Sd C, Watts G, Hughes M, Hannaford J, Dunbar MJ, Laizé CLR, Wilby RL, Battarbee RW, Evans R (2015) Detecting changing river temperatures in England and Wales. Hydrol Process 29:752–766

Perrin AS, Probst A, Probst JL (2008) Impact of nitrogenous fertilizers on carbonate dissolution in small agricultural catchments: implication for weathering CO2 uptake at regional and global scales. Geochim Cosmochim Acta 72:3105–3123

Prasuhn V, Sieber U (2005) Changes in diffuse phosphorous and nitrogen inputs into surface waters in the Rhine watershed in Switzerland. Aquat Sci 67:363–371

Ramakrishna DM, Viraraghavan T (2005) Environmental impact of chemical deicers—a reviw. Water and Soil Pollution 166:49–63

Raymond PA, Cole JJ (2003) Increase in the export of alkalinity from North America's largest river. Science 380:88–91

Raymond PA, Oh N-H, Turner RE, Broussard W (2008) Anthropogenically enhanced fluxes of water and carbon form the Mississippi River. Nature 453:449–452

Raymond PA, Zappa CJ, Butman D, Bott TL, Potter J, Mulholland P, Laursen AE, McDowell WH, Newbold D (2012) Scaling the gas transfer velocity and hydraulic geometry in streams and small rivers. Limnol Oceanogr: Fluids and Environ 2:41–53

Reid PC et al. (2015) Global impacts of the 1980s regime shift. Global change biology

Rodionov SN (2004) A sequential algorithm for testing climate regime shifts. Geophys Res Lett 31:L09204

Rodriguez-Murillo JC, Zobrist J, Fiella M (2015) Temporal trends in organic carbon content in the main Swiss rivers. Sci Total Environ 502:206–217

Rogara M (2007) Synchronous trends in N-NO3 export from N-saturated river catchments in relation to climate. Biogeochem 86:251–268

Ruff M, Singer H, Ruppe S, Mazacek J, Dolf R, Leu C (2013) 20 Jahre Rheinüberwachung. Aqua & Gas 5:16–25

Schuerch M, Kozel R, Schotterer U, Tripet JP (2003) Observation of isotopes in the water cycle—the Swiss National Network (NISOT). Environ Geol 45:1–11

Schwandt D, Deutsch M, Keller M (2010) The beginnings of systematic water quality investigations in the catchments of the rivers Elbe and Rhine—historical situation, protagonists, developments (in German with english summary). Hydrologie und Wassebewirtschaftung 54: 116–128

Siegrist HR, Boller M (1999) Auswirkungen des Phosphatverbots in den Waschmitteln auf die Abwasserrreinigung in der Schweiz. Korrespondenz Abwasser 46:57–65

Spiess E (2011) Nitrogen, phosphorous and potassium balances and cycles of Swiss Agriculture from 1975 to 2008. Nutrient Cycle in Agroecosyst 91:351–365

Stets EG, Kelly VK, Crawford CG (2014) Long-term trends in alkalinity in large rivers of the conterminous US in relation to acidification, agriculture and hydrological modification. Sci Total Environ 488-489:280–289

Stoll JMA, Giger W (1998) Mass balance for detergent-derived fluorescent whitening agents in surface waters of Switzerland. Water Res 32:2041–2050

Stumm W, Morgan JJ (1996) Aquatic chemistry. John Wiley & Sons, New York, p 1022

Szramek K, Walter LM (2004) Impact of carbonate precipitation on riverine inorganic carbon mass transport from a mid-continent forested watershed. Aquat Geochem 10:99–137

Szramek K, Walter LM, Kanduc T, Ogrine N (2011) Dolomite versus calcite weathering in hydrogeochemically diverse watersheds established on bedded carbonates (Sava and Soca Rivers, Slovenia). Aquat Geochem 17:357–396

Team RDC (2011) R. A language and environment for statistical computing. R Foundation for Statistical Computing, Vienna

Webb BW, Nobilis F (2007) Long-term changes in river temperature and the influence of climatic and hydrological factors. Hydrol Sci J 52:74–85

Wessels M, Mohaupt K, Kummerlin R, Lenhard A (1999) Reconstructing past eutrophication trends from diatoms and biogenic silica in the sediment and the pelagic zone of Lake Constance, Germany. J Palelimnol 21:171–192

Worrall F, Howden NJK, Burt TP (2012) A 125 year record of fluvial calcium flux from a temperate catchment: interplay of climate, land-use change and atmospheric deposition. J Hydrol 468-469:249–256

Worrall F, Howden NJK, Burt TP (2013) Assessment of sample frequency bias and precision in fluvial flux calculations—an improved low bias estimation method. J Hydrol 503:101–110

Worrall F, Howden NJK, Burt TP (2015) Time series analysis of the world's longest fluvial nitrate record: evidence for changing states of catchment saturation. Hydrol Process 29:434–444

Zobrist J (2010) Water chemistry of Swiss alpine rivers. In: Bundi U (ed) Alpine waters. Handbook Environmental Chemistry. Springer Verlag, Berlin Heidelberg, pp 95–118

Zobrist J, Reichert P (2006) Bayesian estimation of export coefficients from diffuse and point sources in Swiss watersheds. J Hydrol 329: 207–223

Zobrist J, Sigg L, Schoenenberger U (2004) NADUF - thematische Auswertung der Messresultate 1974 bis 1998. Schriftenreihe der Eawag. Eawag, Duebendorf, p 125

Zobrist J, Schoenenberger U, Alder AC, Kaenel B, Steinmann P, Giger W (2011) 77 Jahre Untersuchungen an der Glatt. Aqu & Gas 315–327

Links

http://ec.europa.eu/environment/water/water-framework/index_en.html

https://pubs.usgs.gov/of/1987/ofr87-242

https://si-ola.inra.fr

https://vminteq.lwr.kth.se

https://www.admin.ch/opc/en/classified-compilation/19910022/index.html

http://www.awel.zh.ch/internet/baudirektion/awel/de/wasser/messdaten/gw_qualitaet.html#s-dosten

https://www.bafu.admin.ch/bafu/de/home/themen/luft/publikationen-studien/publikationen/nabel-luftqualitaet-2016.html

https://www.bafu.admin.ch/bafu/en/home/topics/water/state/water–monitoring-networks/national-surface-water-quality-monitoring-programme–nawa-/national-river-monitoring-and-survey-programme–naduf-.html

https://www.bafu.admin.ch/bafu/de/home/zustand/indikatoren.html

http://www.eawag.ch/en/department/wut/main-focus/chemistry-of-water-resources/naduf/

http://www.eawag.ch/fileadmin/Domain1/Beratung/Beratung_Wissenstransfer/Publ_Praxis/Faktenblaetter/fb_Streusalz_Nov2011.pdf

http://www.emep.int/mscw/mscw_data.html

http://www.iawr.org

https://www.iksr.org/wasserrahmenrichtlinie/bewirtschaftungsplan-2015

http://www.meteoswiss.admin.ch/home/climate/swiss-climate-in-detail/Swiss-temperature-mean/Data-on-the-Swiss-temperature-mean.html

http://www.meteoschweiz.admin.ch/home/klima/klimawandel-schweiz/vegetationsentwicklung/lange-phaenologische-beobachtungsreihen.html